Annals of Operations Research
https://doi.org/10.1007/s10479-023-05568-z

ORIGINAL RESEARCH

The impact of pollution on the dynamics of industry location and residence choice

P. Commendatore[1,2] · **I. Kubin**[3] · **M. Sodini**[1,4] · **I. Sushko**[5]

Received: 17 February 2023 / Accepted: 17 August 2023

Abstract
In this paper we analyze the role of pollution for industry location and residence choice. We present a new economic geography (NEG) model in which manufacturing generates local pollution (that does not accumulate) and uses two types of labour input: unskilled workers that cannot migrate and work where they live; and high-skilled entrepreneurs that choose where to produce and where to live. Taking on board costless commuting or, in alternative, distance working, entrepreneurs can live in a different location from production. Both types of households enjoy utility from consuming all commodities (locally and imported variants) and suffer from local pollution. The resulting model is of the footloose entrepreneur variant, but involves two dynamic equations: the standard one governing the residential choice of entrepreneurs, and another one governing where production is located. The current paper analyses the discrete time dynamic process defined by a two-dimensional piecewise smooth map. Depending on parameters this map can have possibly coexisting attractors of various types (fixed points, cycles, closed curves as well as chaotic attractors). We analytically obtain stability conditions for the fixed points. Using numerical methods we describe also some global dynamic properties of the considered map. Finally, we propose an economic interpretation of the results concerning local stability analysis and global dynamics.

Keywords New economic geography · Environmental pollution · Industry location · Residence choice · Bifurcation analysis · Complex dynamics

JEL Classification C62 · D43 · F12 · F2 · Q50 · R30

✉ P. Commendatore
commenda@unina.it; pasquale.commendatore@unina.it

1 University of Naples 'Federico II', Naples, Italy

2 National Research Council - Institute for Studies on the Mediterannean (Ismed-CNR), Naples, Italy

3 Vienna University of Economics and Business WU, Vienna, Austria

4 Faculty of Economics, Department of Finance, Technical University of Ostrava, Ostrava, Czech Republic

5 Institute of Mathematics, NASU, and Kyiv School of Economics, Kyiv, Ukraine

Published online: 08 September 2023

1 Introduction

Many factors shape the distribution across space and through time of industrial production. Krugman (1993) distinguishes between first nature advantages, depending on natural features, and second nature advantages, caused by human economic activities, as main determinants of industrial agglomeration. The main focus of the new economic geography (NEG) approach is to highlight which type of endogenous economic forces are at the core of the dynamic processes that determine spatial distribution of the economic activities, mostly in the context of a two-region economy. These are named agglomeration and dispersion forces. The agglomeration of industry is spurred by the size of the market (market size effect) – firms are attracted by the region with the higher concentration of consumers / households – and by the cost of living (cost of living effect) – households, which are also factor owners, prefer to live in the region where more goods are available at lower prices; whereas it is discouraged by crowded markets (market competition effect) – firms prefer to locate where competition is less fierce. The balancing of these forces, which are governed by increasing returns and trade costs, determines the long-run distribution of the industrial activity across space: in Krugman (1991) core-periphery (CP) model these are full agglomeration in one region or symmetric dispersion across the regions. The dynamic processes leading to one of these long-run equilibria are one-dimensional and framed in continuous time. In this context, environmental pollution could represent a further dispersion force that may counteract the process of industrial agglomeration (pollution effect) – with households being attracted by a cleaner environment. Indeed, contemporary industrial economies are heavily challenged by environmental issues. As nowadays widely recognized, air pollution has a strong negative impact on human health, on the environment and on human activities (OECD, 2016). Population can escape the damaging effect of pollution by adopting defensive behaviour avoiding air pollution exposure or alleviating the consequences of its effects. In alternative, households may follow Tiebout's (1956) model approach by "voting with their feet", that is, moving to places with the preferred characteristics. A growing empirical literature (see for example Xu and Sylwester (2016); Chen et al. (2022); Li et al. (2020); Xue et al. (2021); Levine et al. (2018); Germani et al. (2021); Heblich et al. (2021) examines the causality link between air pollution and residence choices highlighting that population with higher levels of education is more willing to escape pollution. Migration motivated by the search of cleaner air occurs at different geographical scales involving movements between countries, regions, cities and even within cities. In their study, Xu and Sylwester (2016), looking at migration across countries, show that air pollution is positively associated with population movements, especially considering the highly educated individuals. Individuals may also opt for within-country migration to avoid pollution. Chen et al. (2022), Li et al. (2020) and Xue et al. (2021) show that pollution is an important driver for internal migration in China, one of the countries more exposed to pollution. Their studies reveal that the willingness of households to settle down in the place where they work is negatively affected by the air pollution level in that location. On an even lower scale, Heblich et al. (2021) observe that air pollution affecting cities during the industrial revolution had a well-defined long-term effect on the spatial sorting of low and high-skilled workers within the metropolitan areas in England and Wales. In line with the current empirical literature on the relationship between pollution and residence choices, our analysis tries to capture the idea that people, especially with a high level of education, prefer to live sufficiently far from more polluted areas. As a consequence, residence choices of high skilled workers are necessarily separated from (polluting) firms' location choices. On the other hand, industrial agglomeration often occurs where the local markets are bigger.

It follows that households' residence choices may have a feedback on industrial location decisions by enlarging the local market size (for a concise literature review on the empirical relevance of the market size effect on industrial agglomeration, see Gaspar, 2018). This discussion suggests quite neatly that households' residence choices and (polluting) firms' location decisions are interrelated but do not necessarily coincide.

Some contributions in the NEG literature explore the impact of environmental pollution on industrial location. In one of these, van Marrewijk (2005) introduces pollution in a NEG model – in particular in the footloose entrepreneur (FE) variant developed by Ottaviano (2001) and Forslid and Ottaviano (2003)[1] – as a local negative externality damaging household's welfare. Specifically, this author introduces what is known in the environmental economics literature as 'damage function' as a multiplicative (non separable) term in the utility function (introducing a 'distaste effect' of pollution on consumption; see Michel and Rotillon (1995), for a more detailed definition of this effect). Moreover, he assumes that increasing pollution is related to production in both the industrial sector and in the agricultural (traditional or constant returns) sector. As a consequence, a damaged environment could represent an agglomeration force (rather than a dispersion force) when pollution generated by the agricultural sector has a larger detrimental impact on welfare compared to that of the industrial sector. Lange and Quaas (2007) introduce, in an otherwise similar FE set up where only industrial production generates harmful emissions, the damage function as an additive (separable) non-linear term in the utility function and therefore pollution does not affect the choice over the consumption goods (excluding a distaste effect of pollution on consumption). These authors confirm that, when only industrial pollution is involved, environmental damage represents a dispersion force. They show that, depending on transport costs and environmental damage, several patterns of industrial location are possible. In particular, a flow of local industrial pollution could generate stable partial agglomeration equilibria where the balancing of agglomeration and dispersion forces is such that the industrial sector is not fully agglomerated nor symmetrically dispersed across space but distributed asymmetrically in both regions.

As in Lange and Quaas (2007), Ciucci et al. (2015) introduce the damage function as a separable term in the utility function in an FE model. Ciucci et al. (2015) consider the case of transboundary pollution, when the damaging effects of pollution involves the utility of households living in a place far away from where the emissions originate. These authors conclude that when transboundary pollution is symmetric but most of the damaging effect on utility is local, pollution has a dispersion effect; it follows that the results are analogous to those found in Lange and Quaas (2007); instead, when the damaging effect of pollution emitted in one location mostly involves a different location, pollution represents an agglomeration force, confirming van Marrewijk's (2005) considerations. Finally, when transboundary pollution is asymmetric, new equilibrium configurations could emerge.

In Martínez-García et al. (2022), pollution effects are again local. In their contribution pollution, which increases production, builds up as a stock in each region and it is only partially absorbed by the natural environment. In their CP framework, the agricultural sector has been removed. This eliminates the dispersion force originating from the demand of immobile agricultural workers. Martínez-García et al. (2022) explore the processes concerning factor migration and the regional stocks of pollution. The ensuing three-dimensional dynamics,

[1] In the Krugman (1991) core-periphery model, only one factor, industrial workers, enters in the manufacturing production process both as fixed and variable component. Industrial workers are mobile, while agricultural workers are immobile. In the footloose entrepreneur variant (developed by Ottaviano, 2001, and Forslid and Ottaviano, 2003) the fixed factor component is represented by skilled workers (entrepreneurs); and the variable component is represented by unskilled workers (workers). Only the entrepreneurs are allowed to move across regions.

which is framed in continuous time, may exhibit 'pollute-and-flee' cycles according to which in a first phase population and industry agglomerates in one region and in a second phase, as the stock of pollution increases locally affecting negatively welfare, the migration process is reverted.[2]

In all these contributions factor-owners and firms are tied together. Therefore households and firms mobility are not separate processes. Borck et al. (2010) explore the joint determination of industry location and residence choice as independent processes. In their analysis they consider three cases concerning interregional population mobility: (1) prohibitive commuting costs; (2) zero commuting costs; (3) positive but not prohibitive commuting costs. For the last two cases, Borck et al. (2010) show the possibility of equilibria with separation between the locations of production and residence. In their analysis, however, industry location and residence decisions are not taken simultaneously but in separate phases. The resulting dynamics is not dissimilar from standard NEG models. Moreover, they do not consider the role of environmental issues.

In the NEG literature only a few contributions explore households residence choices and firms mobility decisions as separate processes and how these processes are affected by environmental issues. Examples are Rauscher (2009) and Rauscher and Barbier (2010). In Rauscher (2009) firms and households location decisions are taken separately: firms location is driven by factor remunerations, while households residence choices (in the absence of commuting costs) are driven by utility levels. As in previous contributions households utility levels include a negative externality induced by local industrial pollution emissions. Moreover, in his model, due to the assumption of quasilinear preferences, the demand function does not include the price index (excluding cross-elasticity effects). As a consequence, the dispersion force originating from local market competition is weaker. [3] Depending on pollution damages different types of stationary equilibria are possible, some of them characterized by the separation between residents and industrial production. Moreover, 'chase-and-flee' cycles could emerge according to which households escape from the more agglomerated region searching for a cleaner environment and firms going after the larger market follow consumers. Rauscher and Barbier (2010) use a similar analytical structure dealing with the relationship between industrial agglomeration and biodiversity conservation.

In this paper we provide a rigorous dynamic analysis of a model similar to Rauscher (2009) aiming at clarifying the impact of pollution damage on the dynamics of firms and households location decisions in a two-region spatial economy. With respect to Rauscher (2009), two are the distinguishing features of our analysis: first, we differentiate between two types of households, while in Rauscher (2009) all households are identical. Entrepreneurs (or skilled workers) endowed with human capital and (unskilled) workers endowed with labour. Entrepreneurs do not necessarily work where they live. We assume that they can travel to work with zero commuting costs or, equivalently, that they are allowed to work at distance. (Unskilled) workers are employed and live in the same place, supplying locally a given amount of the factor. They do not commute and are only allowed to work in presence. They are employed and live in the same place. We consider these different levels of mobility and of distance working as a stylized fact that we would like to take on board. On a more technical note, we adopt a footloose entrepreneur framework, that allows us to derive several

[2] There are other contributions in the NEG literature that deal with environmental issues. These are mainly focussing on the role of environmental policies and / or are at the crossroad between new economic geography and urban economics. For example, see Zeng and Zhao (2009), Gaigné et al. (2012), Borck and Pflüger (2019), Pflüger (2021).

[3] Rauscher (2009) demand functions for manufacturing varieties include neither the price index nor the consumer income. As a consequence, also the market size effect is somehow dampened.

analytical results (see below). Second, the dynamics involving firms and households mobility is framed in a two-dimensional (2D) discrete time framework.

We analyze the 2D discrete time dynamics involved by the NEG framework adopted employing the theory of dynamical systems. More specifically, using the corresponding mathematical terminology, the dynamics that we study are defined by a 2D piecewise smooth map T with natural constraints 0 and 1 for the two main variables which are the regional shares of mobile households population (i.e. the entrepreneurs) and firms. Depending on parameters, this map can have attracting fixed points, cycles, closed invariant curves as well as chaotic attractors, and these attractors may coexist. In case of multistability, quite intermingled basins of attraction increase complexity and uncertainty of the dynamics. In the paper, we show that besides the core-periphery fixed points, map T can have interior symmetric and asymmetric fixed points, as well as border fixed points. For all these fixed points, we obtain analytically stability conditions and describe their possible bifurcations. In particular, we give conditions of supercritical, subcritical and degenerate pitchfork bifurcations of the symmetric fixed point, and of its Neimark-Sacker bifurcation leading to an attracting closed invariant curve (with periodic or quasiperiodic dynamics). For the description of degenerate bifurcations we refer to Sushko and Gardini (2010). By means of 1D and 2D bifurcation diagrams we investigate bifurcation scenarios which can be observed under variation of parameter(s). From the nonlinear dynamics perspective, the map is interesting because due to its nonsmoothness, topological attractors may coexist with invariant sets which are attracting in Milnor sense only (see Milnor, 1985). Specifically, we study parameter regions where the core-periphery fixed points are saddles, but they have basins of attraction of positive measure. Similar phenomena also occur in other NEG models, see e.g. Commendatore et al. (2015a, b, 2021). Moreover, these fixed points can coexist with other attracting fixed points, attracting closed invariant curves or with chaotic attractors. One more nonstandard phenomena caused by the nonsmoothness of map T is a transformation of the attracting in Milnor sense core-periphery fixed points into superstable (in topological sense) fixed points, for which the related condition is obtained analytically.

The remainder of the paper is organized as follows: in Sect. 2, we lay down the structure of the economic model; in Sect. 3, we derive the short-run equilibrium solutions; in Sect. 4, we explore the dynamic properties of the model. In particular, we derive the long-run equilibrium solutions, corresponding to the fixed points of the 2D piecewise smooth map T; we verify when these fixed points exist and study their local stability properties. We also look at the global dynamics properties of map T. Finally, we provide an economic interpretation of the results. Section 5 concludes.

2 The economic model

2.1 General set-up

The model setting involves two symmetric regions, region 1 and region 2 ; two sectors, agriculture (A) and manufacturing (M); and two factors of production, labour (L) and human capital (H).

Two types of households live in the economy: (unskilled) workers (L) – endowed with labour – and skilled workers / entrepreneurs (E) – endowed with human capital (H). Workers reside where they work, provide labour locally to A and M and are equally spread between the regions. Thus, $L/2$ is the number of workers located in each region. Entrepreneurs may

work and live in different locations (and we disregard commuting costs between the regions or, equivalently, we assume that they may work at distance), allocating their endowment of H between the regions. Human capital is specific to M. E is the overall number of entrepreneurs and H is the overall endowment of capital. Thus, H/E is the endowment of human capital of each entrepreneur. Moreover, λ is the share of entrepreneurs dwelling in region 1 ($1-\lambda$ in region 2).

In the A sector perfect competition prevails. By choosing the homogeneous good A as the numéraire, from market equilibrium, it follows that workers' wage is equal to 1. Moreover, the A-good is traded without incurring trade costs.

In the M sector monopolistic competition prevails. The production of one of the N varieties of the M-good requires a fixed amount F of human capital and ς units of labour for each additional unit. The cost of trading the M-good between the regions takes the usual iceberg form: $\tau > 1$ units of the good should ship from one region to deliver 1 unit of the good in the other region. Each firm produces a single variety, thus $N = H/F$ is also the overall number of firms. N_1 is located in region 1 and N_2 in region 2, with $N = N_1 + N_2$. We denote by η the share of human capital allocated in region 1 ($1-\eta$ in region 2). Thus $N_1 = \eta H/F$ corresponds to the number of firms located in region 1 and $N_2 = (1-\eta)H/F$ to the number of firms located in region 2. It follows that η is also the share of firms located in region 1 ($1-\eta$ in region 2).

2.2 Consumption

2.2.1 General utility function

The representative consumer utility function is:

$$u(c_M, c_A, \varepsilon) = \upsilon(c_M, c_A) - D(\varepsilon) \tag{1}$$

The component $\upsilon(c_M, c_A)$ describes the choice between the manufacturing good and the agricultural good, where c_M is the consumption of a composite of manufacturing good varieties and c_A is the consumption of the agricultural good. The component $D(\varepsilon)$ is additive and describes the negative impact on utility of industrial pollution emissions, ε. We are assuming that pollution emissions do not affect the enjoyment of the other goods. That is, there is not a 'distaste effect' of pollution on consumption.

2.2.2 Damage function

We use the following damage function, which specifies how total damage, caused by industrial emissions ε, affects consumer's utility (see Rauscher, 2009):

$$D(\varepsilon) = \frac{\delta \varepsilon^{1+z}}{1+z} \tag{2}$$

where $\delta \geq 0$ represents the intensity of the pollution effect on utility and $z > 0$ shapes the damage function. Let $\varepsilon > 0$ and $\delta > 0$, we have that: $D' = \delta \varepsilon^z > 0$, $D'' = z\delta\varepsilon^{z-1} > 0$ and $D''' = z(z-1)\delta\varepsilon^{z-2} \geq (<0)\ for\ z \geq (<1)$. From the last expression, the marginal damage function D' is convex, concave or linear depending on $z > 1$, $z < 1$ or $z = 1$, respectively. Typically in environmental economics $D' \geq 0$ is the standard assumption. As in Rauscher (2009), we consider also the case of a concave marginal damage function, this will allow us

to focus on the impact of the damage function curvature on the dynamic properties of the model.

Notice that, as in other contributions (see Lange & Quaas, 2007, and Rauscher, 2009) we assume that pollution originates only from the industrial sector, does not accumulate over time and has only local effects.

2.2.3 Individual consumer maximization problem

The utility component concerning the choice between manufacturing varieties and the agricultural good, $\upsilon(c_M, c_A)$, is quasilinear with the manufacturing good component represented by a monotonic transformation of a CES:

$$\upsilon(c_M, c_A) = c_M + c_A \tag{3}$$

where

$$c_M = \theta \frac{\sigma}{\sigma - 1} \left(\sum_{i=1}^{N} c_i^{\frac{\sigma-1}{\sigma}} \right) \tag{4}$$

and where c_i corresponds to the consumption of variety i, with $i = 1, ..., N$. Moreover, $\theta > 0$ and $\sigma > 1$.

The budget constraint of a representative consumer (worker or entrepreneur) corresponds to:

$$\sum_{i=1}^{N} p_i c_i + p_A c_A = Y + p_A \overline{c_A} \tag{5}$$

where p_i corresponds to the price of variety i, with $i = 1, ..., N$, p_A is the price of the A-good and $\overline{c_A}$ is a given endowment of the A-good. In this expression, $\sum_{i=1}^{N} p_i c_i$ and $p_A c_A$ represent the expenditures for the manufacturing varieties and for the agricultural good, respectively; Y the consumer (worker or entrepreneur) income and $p_A \overline{c_A}$ the value of her endowment of the A-good.

Solving the utility maximization problem subject to the budget constraint, after choosing the agricultural good as the numéraire, $p_A = 1$, we obtain:

$$c_i = \frac{\alpha}{p_i^{\sigma}}$$

where we set $\alpha = \theta^{\sigma}$. Note that, since we are not yet considering production location, we are not distinguishing in this expression between the price of a variety produced locally and the price of an imported variety.

2.3 Production

The structure of production follows the footloose entrepreneur framework (see Ottaviano, 2001, and Forslid & Ottaviano, 2003) according to which the mobile factor (human capital) enters in the production only as the fixed component. The profit of a representative firm is

$$\pi = pq - (\varsigma q w_L + F w)$$

where q is the output, ς, as specified above, is the variable input requirement, F is the fixed amount of human capital required for production, w_L is the unskilled workers nominal wage and w is the human capital remuneration.

We now introduce geography and symmetric firms behavior. Considering that from perfect competition in the agricultural market: $w_L = p_A = 1$, profits of a representative firm located in region 1 or in region 2 are given by:

$$\pi_1 = p_{11}Q_{11} + p_{12}\tau Q_{12} - [\varsigma(Q_{11} + \tau Q_{12}) + Fw_1] \tag{6}$$
$$\pi_2 = p_{22}Q_{22} + p_{21}\tau Q_{21} - [\varsigma(Q_{22} + \tau Q_{21}) + Fw_2] \tag{7}$$

where p_{ij} is the "mill" price (i.e., which excludes transport costs) applied in region j by a firm located in region i, Q_{ij} is the quantity sold in region j by a firm located in region i, with $i, j = 1, 2$;[4] and where, as mentioned above, $\tau > 1$ represents iceberg trade costs and, for future reference, $\phi = \tau^{1-\sigma}$, represents trade freeness, with $0 \leq \phi < 1$.

The market equilibrium conditions in the manufacturing goods markets are:

$$Q_{11} = c_{11}\left(\frac{L}{2} + \lambda E\right); \quad Q_{12} = c_{12}\left(\frac{L}{2} + (1-\lambda)E\right)$$
$$Q_{21} = c_{21}\left(\frac{L}{2} + \lambda E\right); \quad Q_{22} = c_{22}\left(\frac{L}{2} + (1-\lambda)E\right)$$

To simplify the notation we set $\varsigma = \frac{\sigma-1}{\sigma}$. Then, we replace the above conditions into the expressions for the regional profits and taking into account that prices at destination include trade costs:[5]

$$c_{11} = \alpha p_{11}^{-\sigma}, \quad c_{12} = \alpha p_{12}^{-\sigma}\tau^{-\sigma} \tag{8}$$
$$c_{21} = \alpha p_{21}^{-\sigma}\tau^{-\sigma}, \quad c_{22} = \alpha p_{22}^{-\sigma}, \tag{9}$$

we obtain the following profit maximizing (mill) prices: $p_{ij} = 1$ with $i, j = 1, 2$.

2.4 Pollution

Assumed that pollution is proportional to production: for each unit of output ψ units of pollution are emitted. Then, the quantity of emissions in the two regions is equal to:

$$\varepsilon_1 = \psi N_1 Q_1 \tag{10}$$
$$\varepsilon_2 = \psi N_2 Q_2 \tag{11}$$

where $Q_1 = Q_{11} + \tau Q_{12}$ and $Q_2 = \tau Q_{21} + Q_{22}$.

[4] Note that in the NEG literature more often are used prices at delivery which includes transport costs rather than prices at the origin or "mill" prices (this distinction is equivalent to that between FOB ("free-on-board") and CIF ("cost-insurance- and -freight") prices used in international economics. Defining $\widetilde{p}_{12} = p_{12}\tau$ and $\widetilde{p}_{21} = p_{21}\tau$ Eqs. (6) and (7) correspond to:

$$\pi_1 = p_{11}Q_{11} + \widetilde{p}_{12}Q_{12} - [\varsigma(Q_{11} + \tau Q_{12}) + Fw_1]$$
$$\pi_2 = p_{22}Q_{22} + p_{21}\tau Q_{21} - [\varsigma(Q_{22} + \tau Q_{21}) + Fw_2]$$

[5] Referring also to the previous footnote, in these expressions, we have taken into consideration that the price at destination (CIF price) for a variety produced in region i and purchased in region j is: $\widetilde{p}_{ij} = p_{ij}\tau$, with $i, j = 1, 2$ and $i \neq j$.

3 Short-run equilibrium

A short-run equilibrium is such that goods and factors markets are simultaneously in equilibrium for a given spatial distribution of households and firms as determined by λ and η, respectively. In the following, we identify regional human capital remunerations and entrepreneurs indirect utilities that ensure such an equilibrium. As we shall see, the remuneration and utility differentials are at the core of the long-run dynamics.

3.1 Human capital regional remunerations

From the zero profit conditions (obtained by setting $\pi_1 = 0$ and $\pi_2 = 0$ in (6) and (7)), after replacing for the profit maximizing prices, we obtain the short-run equilibrium values for the regional human capital remunerations:

$$w_1 = \frac{1}{\sigma F} Q_1 = \frac{\alpha}{\sigma F}\left[\frac{L}{2} + \lambda E + \phi\left(\frac{L}{2} + (1-\lambda)E\right)\right] \tag{12}$$

$$w_2 = \frac{1}{\sigma F} Q_2 = \frac{\alpha}{\sigma F}\left[\phi\left(\frac{L}{2} + \lambda E\right) + \frac{L}{2} + (1-\lambda)E\right] \tag{13}$$

The terms in square brackets indicate the market size that determines not only human capital remunerations but also output levels of single firms. Note that due to transport costs market size depends upon the regional distribution of the consumers, i.e. upon λ.

3.2 Entrepreneurs regional indirect utilities

From (1) and (3), the utility enjoyed by a representative entrepreneur living in region 1 or in region 2 is

$$u_1(c_{M,1}, c_A, \varepsilon_1) = c_{M,1} + c_A - D(\varepsilon_1)$$
$$u_2(c_{M,2}, c_A, \varepsilon_2) = c_{M,2} + c_A - D(\varepsilon_2)$$

where from (4),

$$c_{M,1} = \theta \frac{\sigma}{\sigma - 1}\left(N_1 c_{11}^{\frac{\sigma-1}{\sigma}} + N_2 c_{21}^{\frac{\sigma-1}{\sigma}}\right)$$
$$c_{M,2} = \theta \frac{\sigma}{\sigma - 1}\left(N_1 c_{12}^{\frac{\sigma-1}{\sigma}} + N_2 c_{22}^{\frac{\sigma-1}{\sigma}}\right)$$

and from (2),

$$D(\varepsilon_1) = \frac{\delta \varepsilon_1^{1+z}}{1+z}$$
$$D(\varepsilon_2) = \frac{\delta \varepsilon_2^{1+z}}{1+z}$$

Replacing for utility maximizing consumption, considering (8) and (9) and that $p_{ij} = 1$ $(i, j = 1, 2)$, $\alpha = \theta^\sigma$, $N_1 = \eta \frac{H}{F}$ and $N_2 = (1-\eta)\frac{H}{F}$, the indirect utilities correspond to

$$u_1 = \alpha \frac{\sigma}{\sigma - 1}\frac{H}{F}\left(\eta + \phi(1-\eta)\right) + c_A - \frac{\delta \varepsilon_1^{1+z}}{1+z} \tag{14}$$

$$u_2 = \alpha \frac{\sigma}{\sigma - 1} \frac{H}{F} (\phi\eta + 1 - \eta) + c_A - \frac{\delta \varepsilon_2^{1+z}}{1+z} \tag{15}$$

Note that the first component of the indirect utilities (referring to the consumption of the manufacturing good) depends also on the distribution of firms between the region. The higher the share of locally available variants (that do not involve transport cost and, therefore, are cheaper), the higher the utility. We refer to this as cost of living effect.

Using the budget constraint (5) solved for c_A; and expressions (10), (11), (12), (13), (14) and (15), we obtain

$$u_1 = \frac{H}{E}\overline{w} + \overline{c_A} + \alpha \frac{1}{\sigma - 1} \frac{H}{F} (\eta + \phi(1 - \eta)) - \frac{\delta}{1+z} (\eta H \sigma \psi w_1)^{1+z}$$
$$u_2 = \frac{H}{E}\overline{w} + \overline{c_A} + \alpha \frac{1}{\sigma - 1} \frac{H}{F} (\phi\eta + (1 - \eta)) - \frac{\delta}{1+z} ((1 - \eta)\psi H \sigma w_2)^{1+z}$$

where $\overline{w} = \eta w_1 + (1 - \eta) w_2$ represents the average remuneration of a unit of human capital.

4 Dynamics

4.1 The map

The map summarizing the dynamic model is given below in Eq. (16). It is two-dimensional (2D for short) and it explains how the shares of mobile households (λ) and firms (η) locate between the two regions. The dynamics follows a mechanism similar to the replicator dynamics, which is widely used in evolutionary game theory and which is standard in NEG models (see e.g. Weibull 1995, and Fujita et al. 1999). The share of households living in region 1 (and in region 2) changes on the basis of a comparison between the utility enjoyed in region 1, u_1, and the average utility enjoyed across the economy, $\overline{u}$. The corresponding expression is

$$f(\lambda, \eta) = \lambda \left(1 + \gamma_\lambda \Omega(\lambda, \eta)\right)$$

where $\Omega(\lambda, \eta) = \frac{u_1 - \overline{u}}{\overline{u}}$, $\overline{u} = \lambda u_1 + (1 - \lambda) u_2$ and γ_λ is the speed of adjustment: the higher γ_λ, the stronger households react to differences in regional utility levels. Similarly, the share of human capital allocated by entrepreneurs in region 1 (and in region 2), determining at the same time the shares of firms located in each region, is modified following a comparison between human capital remuneration in region 1, w_1, and the average human capital remuneration across the economy, $\overline{w}$. The corresponding expression is

$$g(\lambda, \eta) = \eta \left(1 + \gamma_\eta \Psi(\lambda, \eta)\right)$$

where $\Psi(\lambda, \eta) = \frac{w_1 - \overline{w}}{\overline{w}}$, $\overline{w} = \eta w_1 + (1 - \eta) w_2$ and, again, γ_η denotes the corresponding speed of adjustment. After introducing the usual constraints on shares, we express the dynamic model as a 2D piecewise smooth map $T : U \to U$, $U = [0, 1] \times [0, 1] \subset \mathbb{R}^2$:

$$T : (\lambda, \eta) \to (F(\lambda, \eta), G(\lambda, \eta)) \tag{16}$$

where

$$F(\lambda, \eta) = \begin{cases} 0 & \text{if } f(\lambda, \eta) \leq 0 \\ f(\lambda, \eta) & \text{if } 0 < f(\lambda, \eta) < 1 \\ 1 & \text{if } f(\lambda, \eta) \geq 1 \end{cases}$$

$$G(\lambda,\eta)=\begin{cases}0 & \text{if } g(\lambda,\eta)\le 0\\ g(\lambda,\eta) & \text{if } 0<g(\lambda,\eta)<1\\ 1 & \text{if } g(\lambda,\eta)\ge 1\end{cases}$$

4.2 Fixed points

As it usually occurs in the NEG models with constraints on the shares, the fixed points of the map T can be classified into two groups, namely, *border* and *interior fixed points*. The first group is associated with the borders of the unit square U and includes

(1) the corner points of U, called *core-periphery (CP) fixed points*, $CP_{00}=(0,0)$, $CP_{11}=(1,1)$, $CP_{01}=(0,1)$, $CP_{10}=(1,0)$, which obviously always exist; in our case, at the fixed points CP_{00} and CP_{11} there is no separation between households and firms, while at CP_{01}, CP_{10} there is a separation;
(2) fixed points belonging to the interior of the borders of U; as we show below, map T can have *border fixed points,* say B and B' (which are necessarily symmetric to each other) belonging to the interior of horizontal borders of U: $B\in\{(\lambda,\eta):0<\lambda<1,\eta=1\}$ and $B'\in\{(\lambda,\eta):0<\lambda<1,\eta=0\}$.

The second group of the fixed points of T is related to the *interior* of U and includes

(3) interior symmetric fixed point, say, $S=(0.5,0.5)$;
(4) interior asymmetric fixed points, say I and I'; below we show that if they exist, they necessarily belong to the vertical segment $\{(\lambda,\eta):\lambda=0.5,\ 0<\eta<1\}$, that is, $\lambda=0.5$ at both fixed points.

Now let us give more details starting from the interior fixed points, namely the fixed points, S, I and I'. From $f(\lambda,\eta)=\lambda$, $g(\lambda,\eta)=\eta$, we get that an interior fixed point satisfies

$$\begin{cases}w_1(\lambda)=w_2(\lambda)\\ u_1(\lambda,\eta)=u_2(\lambda,\eta)\end{cases}$$

The first equation corresponds to

$$\frac{\alpha E(1-\phi)}{\sigma F}(2\lambda-1)=0$$

and it is obviously solved by $\lambda=0.5$. Therefore an interior fixed point must necessarily lie on the vertical segment $\{(\lambda,\eta):\lambda=0.5,\ 0<\eta<1\}$. By setting $\lambda=0.5$ into the second equation, we obtain

$$(2\eta-1)\kappa_1-\delta\frac{\kappa_2^{1+z}\left[\eta^{1+z}-(1-\eta)^{1+z}\right]}{1+z}=0 \tag{17}$$

where

$$\kappa_1=\frac{\alpha H(1-\phi)}{F(\sigma-1)}>0,\quad \kappa_2=\frac{1}{2}\frac{\psi H(1+\phi)(E+L)}{F}>0$$

One of the solutions of (17) is clearly $\eta=0.5$, that leads to the interior symmetric fixed point $S=(0.5,0.5)$ (which always exists). Suppose now that $\eta\neq 0.5$. If z is a natural number, then the Eq. (17) can be written as

$$(2\eta-1)\left[\kappa_1-\frac{\delta}{1+z}\kappa_2^{1+z}\sum_{n=0}^{z}\eta^{z-n}(1-\eta)^n\right]=0 \tag{18}$$

- If $z = 1$, then the Eq. (18) becomes

$$(2\eta - 1)\left(\kappa_1 - \delta\frac{\kappa_2^2}{2}\right) = 0$$

and if $\kappa_1 - \delta\frac{\kappa_2^2}{2} \neq 0$, then only the symmetric fixed point exists, while if $\kappa_1 - \delta\frac{\kappa_2^2}{2} = 0$, i.e. $\delta = \frac{2\kappa_1}{\kappa_2^2}$, then any point of the segment $\{(\lambda, \eta) : \lambda = 0.5,\ 0 < \eta < 1\}$ is a fixed point (as we discuss later, this case corresponds to a *degenerate pitchfork bifurcation* of the fixed point S).
- If $z = 2, 3, \ldots$, then the η-coordinates of the interior fixed points I and I', say, $\eta = \eta^*$ and $\eta = 1 - \eta^*$, correspond to the two real solutions that satisfy Eq. (18) when $\eta \neq 0.5$, which exist only when

$$\delta < \overline{\delta} = \frac{2^z\kappa_1}{\kappa_2^{1+z}} \tag{19}$$

In fact, as we show in Appendix, the condition $\delta = \overline{\delta}$ is related to a (supercritical) pitchfork bifurcation of S leading to two interior fixed points I and I'. Moreover, the η-coordinates of I and I' belong to the unit interval, that is, $0 < \eta^* < 1$, if δ is sufficiently close to $\overline{\delta}$. As we report later, it holds for $\delta > \widetilde{\delta}_2$, where the condition $\delta = \widetilde{\delta}_2$ is associated with a border transcritical bifurcation at which I and I' merge with B and B', respectively, see (21). That is, in this case, the existence condition for I and I' is $\widetilde{\delta}_2 < \delta < \overline{\delta}$.
- If z is not a natural number, the fixed points I and I' can be found numerically only.

Now let us turn to the border fixed points. Considering first the interior of the vertical borders of U, that is, $\{(\lambda, \eta) : \lambda = 0, 0 < \eta < 1\}$ and $\{(\lambda, \eta) : \lambda = 1, 0 < \eta < 1\}$, we get that the condition $w_1(\lambda) = w_2(\lambda)$ is never satisfied for $\lambda = 1$ or $\lambda = 0$, thus, no fixed point can exist located on these borders. For an economic intution (which applies also to the impossibility of an interior equilibrium with asymmetric shares of households, that is, outside the segment $\lambda = 0.5$) note that the regional remunerations of human capital (see Eqs. (12) and (13)) depend upon the regional distribution of demand, weighted by the transport cost. If demand is concentrated in one region, $\lambda = 0$ or $\lambda = 1$, or asymmetrically distributed, firms are faced with different demand conditions, which necessarily translates into different remunerations. Demand conditions are only equal, if demand is symmetrically distributed between the two regions, i.e. for $\lambda = 0.5$. Then, considering the interior of the horizontal borders of U, by setting $\eta = 1$ ($\eta = 0$) in the condition $u_1(\lambda, \eta) = u_2(\lambda, \eta)$, we solve for the λ-coordinates of two border asymmetric fixed points $B = (\lambda^{**}, 1)$ and $B' = (1 - \lambda^{**}, 0)$:

$$\lambda^{**} = \frac{1}{2} + \kappa_3\left(\left(\kappa_1\frac{1+z}{\delta}\right)^{\frac{1}{1+z}}\frac{1}{\kappa_2} - 1\right)$$

$$1 - \lambda^{**} = \frac{1}{2} - \kappa_3\left(\left(\kappa_1\frac{1+z}{\delta}\right)^{\frac{1}{1+z}}\frac{1}{\kappa_2} - 1\right)$$

where

$$\kappa_3 = \frac{1+\phi}{1-\phi}\left(\frac{E+L}{2E}\right) > \frac{1}{2}$$

It can be shown that the existence conditions of B and B', i.e. $0 < \lambda^{**} < 1$, are satisfied for $\widetilde{\delta}_3 < \delta < \widetilde{\delta}_1$, more precisely,

- $0.5 < \lambda^{**} < 1$, for $\widetilde{\delta}_3 < \delta < \widetilde{\delta}_2 < \widetilde{\delta}_1$, where

$$\widetilde{\delta}_1 = (1+z)\kappa_1 \left(\frac{\kappa_3}{\kappa_2(\kappa_3 - 0.5)} \right)^{1+z} \tag{20}$$

$$\widetilde{\delta}_2 = (1+z)\kappa_1 \left(\frac{1}{\kappa_2} \right)^{1+z} \tag{21}$$

$$\widetilde{\delta}_3 = (1+z)\kappa_1 \left(\frac{\kappa_3}{\kappa_2\,(\kappa_3 + 0.5)} \right)^{1+z} \tag{22}$$

- $0 < \lambda^{**} < 0.5$ for $\widetilde{\delta}_3 < \widetilde{\delta}_2 < \delta < \widetilde{\delta}_1$, and
- $\lambda^{**} = 0.5$ for $\delta = \widetilde{\delta}_2$. In this way, at $\delta = \widetilde{\delta}_1$ it holds that $\lambda^{**} = 1$, that is, $B = CP_{11}$ (and $B' = CP_{00}$), while at $\delta = \widetilde{\delta}_3$ it holds that $\lambda^{**} = 1$, that is, $B = CP_{01}$ (and $B' = CP_{10}$). These conditions are related to border transcritical bifurcations at which the border fixed points B and B' appear / disappear merging with the related CP fixed points, changing their stability (in the horizontal direction). At $\delta = \widetilde{\delta}_2$, one more border transcritical bifurcation occurs at which the interior fixed points I and I' appear / disappear merging with B and B', respectively, changing their stability (in the vertical direction).

Note that

$$\frac{d\lambda^{**}}{d\delta} = -\frac{\delta^{-\frac{2+z}{1+z}}}{1+z}\kappa_3 \widetilde{\delta}_2^{\frac{1}{1+z}} < 0$$

for $\delta \neq 0$. This means that when firms are agglomerated in one region, households are attracted by the region with no industry as the damage from pollution increases.

A detailed local stability analysis of the fixed points of map T is presented in Appendix. The bifurcation conditions, that we will use in our numerical analysis, are the following:

(1) the conditions $\delta = \overline{\delta}$ and $\delta = \delta_{NS}$, given in (19) (see also (30)) and (29), respectively, are related to pitchfork and Neimark-Sacker bifurcations of the fixed point S;

(1) the condition $\delta = \widetilde{\delta}_2$, where $\widetilde{\delta}_2$ is given in (20), is associated with a border transcritical bifurcation (in the vertical direction) of the fixed points B and B';

(2) the condition $\delta = \widetilde{\delta}_3$, where $\widetilde{\delta}_3$ is given in (22), corresponds to a border transcritical bifurcation (in the horizontal direction) of the fixed points CP_{00} and CP_{11}.

4.3 Numerical analysis

We complete the exploration of the properties of fixed points of map T with the help of numerical simulations. For the parameter values

$$\sigma = 3,\ E = 1,\ H = 1,\ L = 2,\ F = 0.05,\ \alpha = 0.1,\ \psi = 1,\ \gamma_\lambda = 2,\ \gamma_\eta = 2,\ \overline{c_A} = 0.1 \tag{23}$$

we plot in Fig. 1 the bifurcation curves obtained above in the (ϕ, δ)-parameter plane for $z = 0.5$ in (a), $z = 1$ in (b) and $z = 2$ in (c). In these figures, the curve defined by $\delta = \widetilde{\delta}_3$ is marked by $BT(CP)$ being associated with a border transcritical bifurcation of the fixed points CP_{00} and CP_{11}; the curves defined by $\delta = \overline{\delta}$ and $\delta = \delta_{NS}$, confining the stability domain of the fixed point S and denoted $PF(S)$ and $NS(S)$, respectively, are related to the pitchfork and Neimark-Sacker bifurcations of the fixed point S; the curve denoted $BT(B)$ and defined by $\delta = \widetilde{\delta}_2$ is associated with the border transcritical bifurcation of the fixed points B and B'. In the following, we use the results of the stability analysis of the fixed points presented in Appendix.

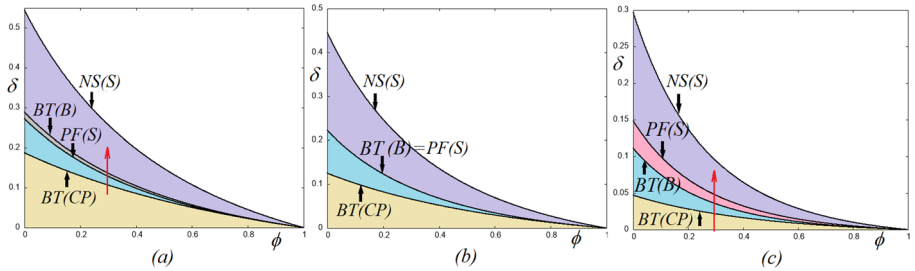

Fig. 1 Bifurcation curves of the fixed points of map T in the (ϕ, δ) -parameter plane for $z = 0.5$ in (**a**), $z = 1$ in (**b**) and $z = 2$ in (**c**). The other parameter values are as in (23)

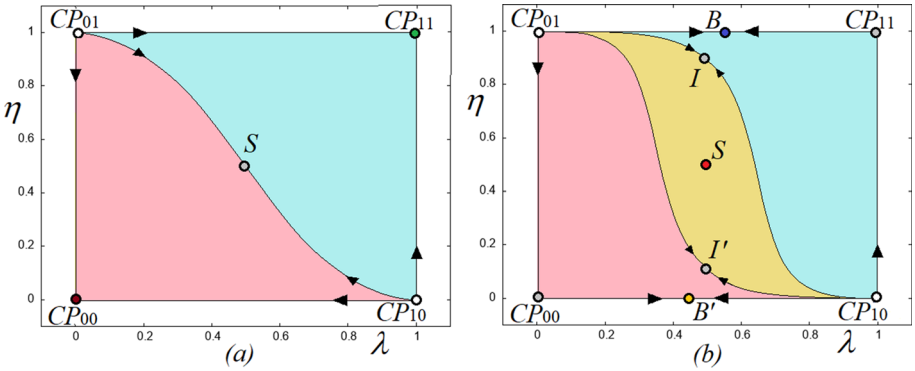

Fig. 2 Basins of attraction of the fixed points **(a)** CP_{00} and CP_{11}, **(b)** S, B and B'. Here $z = 0.5$, $\phi = 0.3$ and (**a**) $\delta = 0.1$; (**b**) $\delta = 0.1325$. The other parameter values are fixed as in (23)

In fact, the fixed points CP_{00} and CP_{11} are locally stable for $0 \le \delta < \widetilde{\delta}_3$, i.e., below the curve $BT(CP)$ (see Fig. 1). Their basins of attraction are separated by the stable invariant manifold of the saddle fixed point S (see an example in Fig. 2a). At $\delta = \widetilde{\delta}_3$, the fixed points CP_{00} and CP_{11} lose stability (in the horizontal direction) via a border transcritical bifurcation leading to two attracting border fixed points, B and B', respectively. Their basins are also separated by the stable invariant manifold of S. These fixed points are stable for $\widetilde{\delta}_3 < \delta < \widetilde{\delta}_2$, i.e. between the curves $BT(CP)$ and $BT(B)$. Concerning the interior symmetric fixed point S, it is stable for $\overline{\delta} < \delta < \delta_{NS}$, that is between the curves $PF(S)$ and $NS(S)$.

The pitchfork bifurcation of S is subcritical for $z < 1$ (as e.g., in Fig. 1a where $z = 0.5$). In this case, crossing $PF(S)$ for increasing δ, the fixed point S becomes stable while two interior saddle fixed points, I and I' are born. Since $\overline{\delta} < \widetilde{\delta}_2$,[6] that is, the curves $PF(S)$ is below the curve $BT(B)$, in the region between these curves three attracting fixed points coexist, namely, S, B and B'. Their basins are separated by the stable invariant manifolds of the saddle fixed points I and I' (see an example in Fig. 2b). For further increasing δ, a reverse border transcritical bifurcation occurs at which I collides with B and I' with B', and after this bifurcation the fixed points I and I' disappear while the border fixed points B and B' become saddles. This sequence of bifurcations is also illustrated in Fig. 3 presenting a bifurcation diagram varying δ in the range $0.08 < \delta < 0.2$ fixing $\phi = 0.3$. The related parameter path in shown in Fig. 1a by a red arrow.

[6] Note that $\overline{\delta} = \widetilde{\delta}_2 \frac{2^z}{1+z}$, thus $\overline{\delta} \ge (<) \widetilde{\delta}_2$ for $z \ge (<) = 1$.

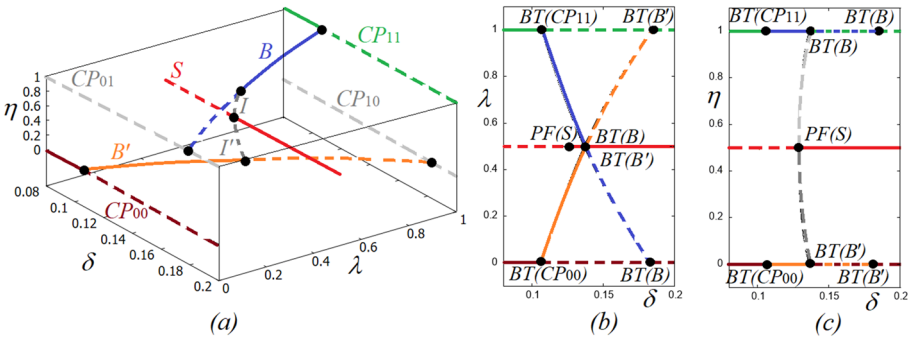

Fig. 3 Bifurcation diagram **(a)** δ vs λ and η; **(b)** δ vs λ; **(c)** δ vs η. Here $z = 0.5$, $\phi = 0.3$ and $0.08 < \delta < 0.2$ (see the parameter path indicated in Fig. 1a by red arrow). The other parameter values are as in (23)

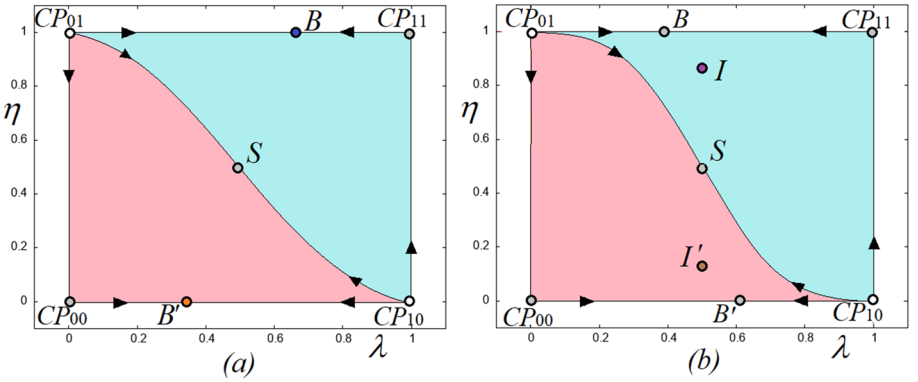

Fig. 4 Basins of attraction of the fixed points **(a)** B and B', **(b)** I and I'. Here $z = 2$, $\phi = 0.3$ and **(a)** $\delta = 0.03$; **(b)** $\delta = 0.04$. The other parameter values are fixed as in (23)

If $z = 1$, the pitchfork bifurcation of S is degenerate (the curves $PF(S)$ and $BT(B)$ coincide, see Fig. 1b), and at the bifurcation value any point of the segment $\{(\lambda, \eta) : \lambda = 0.5,\ 0 \le \eta \le 1\}$ is fixed.

For $z > 1$, the pitchfork bifurcation of S is supercritical (as in Fig. 1c where $z = 2$). In the region between the curves between $BT(CP)$ and $BT(B)$ map T has attracting border fixed points B and B' whose basins are separated by the stable invariant manifold of saddle fixed point S (an example is shown in Fig. 4a). Crossing $BT(B)$ for increasing δ, a border transcritical bifurcation of B and B' transforms them into saddles and leads to interior attracting fixed points I and I' (see Fig. 4b). As δ is further increased, at $\delta = \overline{\delta}$, (i.e., crossing the curve $PF(S)$), a reverse supercritical pitchfork bifurcation occurs due to which the fixed points I and I' disappear merging with the symmetric interior equilibrium S gaining stability. This sequence of bifurcations is illustrated in Fig. 5 presenting a bifurcation diagram varying δ in the range $0 < \delta < 0.08$ fixing $\phi = 0.3$. The related parameter path in shown in Fig. 1c by a red arrow.

Finally, at $\delta = \delta_{NS}$ (crossing the curve $NS(S)$, see Fig. 1), the fixed point S loses stability via a Neimark-Sacker bifurcation. This bifurcation leads to the appearance of an attracting closed invariant curve with periodic or quasiperiodic dynamics on it. In the next section we consider several examples of dynamics of map T for $\delta > \delta_{NS}$.

4.4 Global dynamics

In Fig. 6a we the present bifurcation structure in the (ϕ, δ) -parameter plane of map T for $z = 0.5$. In this figure, the white region is related to either quasiperiodic, or periodic or chaotic dynamics with possibly coexisting attractors. Some periodicity tongues issuing from the Neimark-Sacker bifurcation curve can be better seen in the inset which shows the marked window magnified (periods of the corresponding cycles are indicated by numbers). In Fig. 6a one more curve denoted C is shown associated with a vertical asymptote $\lambda = \lambda_a$ of function $f(\lambda)$ given in (31) in Appendix, which for parameter values above C belongs to the unit interval. This curve is defined by the condition of vanishing denominator of $f(\lambda)$ at $\lambda = 1$, that leads to the condition $u_1(1) = 0$. Below we discuss the dynamic effects of crossing this curve. Neimark-Sacker bifurcation of the fixed point S is illustrated in Fig. 6b by means of a 1D bifurcation diagram plotting δ versus λ fixing $\phi = 0.15$ and varying δ in the range $0.37 < \delta < 0.42$. In this diagram, several periodicity regions can be seen, in particular, the biggest one corresponding to a 14-cycle which in its turn also undergoes a Neimark-Sacker bifurcation leading to 14 -cyclic attracting closed invariant curves.

Several properties are worth to be commented. The first one is related to the symmetry of the map T with respect to the point S, according to which any invariant set A of T is either itself symmetric with respect to S (e.g., an even period cycle may be symmetric), or there must exist one more invariant set A' which is symmetric to A. It follows that cycles of odd periods must exist in pairs and, as an example, basins of two coexisting 15-cycles are shown in yellow and blue in Fig. 7.

Figure 7b which is an enlargment of the window indicated in Fig. 7a, illustrates one more property of map T, related to its piecewise smooth definition with flat branches. One can see that besides the two attracting 15-cycles, also the fixed points CP_{00} and CP_{11} are attractors of map T with their basins of attraction shown in violet and green. However, we know that these fixed points are saddles for the considered parameter values, being locally repelling in the horizontal direction and attracting in the vertical direction. For the fixed point CP_{11} this fact is illustrated in Fig. 8 by the related 1D maps denoted $T_{\eta=1}(\lambda)$ in (a) and $T_{\lambda=1}(\eta)$ in (b) to which map T is reduced on the invariant borders $\{(\lambda, \eta) : \eta = 1,\ 0 \le \lambda \le 1\}$ and $\{(\lambda, \eta) : \lambda = 1,\ 0 \le \eta \le 1\}$, respectively. The same property holds for the fixed point CP_{00} on the invariant borders $\{(\lambda, \eta) : \eta = 0,\ 0 \le \lambda \le 1\}$ and $\{(\lambda, \eta) : \lambda = 0,\ 0 \le \eta \le 1\}$. In

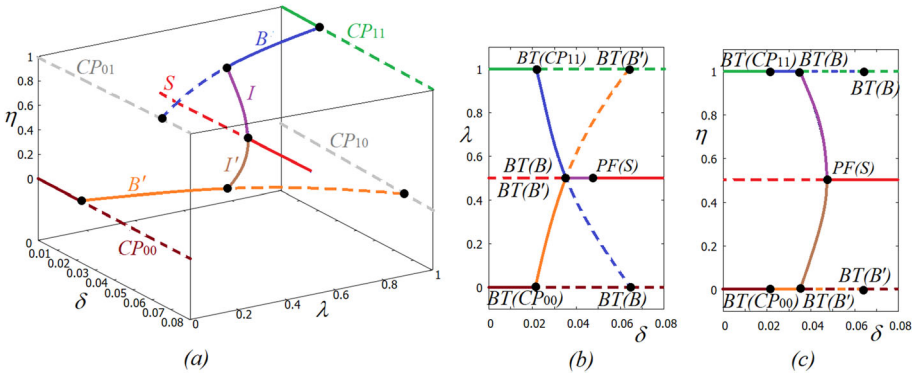

Fig. 5 Bifurcation diagram **(a)** δ vs λ and η; **(b)** δ vs λ; **c** δ vs η. Here $z = 2$, $\phi = 0.3$ and $0 < \delta < 0.08$ (see the parameter path indicated in Fig. 1(c) by red arrow). The other parameter values are as in (23)

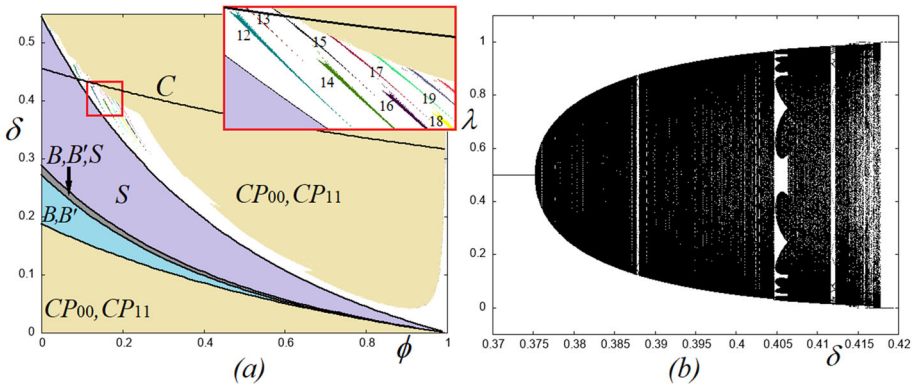

Fig. 6 **(a)** Bifurcation structure in the (ϕ, δ) -parameter plane of map T for $z = 0.5$. An inset shows the marked window magnified. **(b)** 1D bifurcation diagram δ versus λ for $\phi = 0.15$ and $0.37 < \delta < 0.42$. The other parameter values are fixed as in (23)

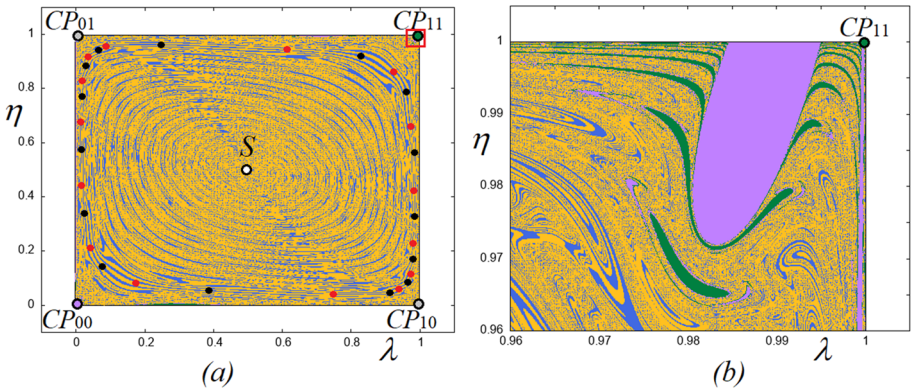

Fig. 7 **(a)** Basins of two attracting symmetric 15-cycles coexisting with attracting (in Milnor sense) fixed points CP_{00} and CP_{11} are shown in yellow, blue, violet and green, respectively. **(b)** A magnified window indicated in (**a**) where the basins of CP_{00} and CP_{11} are more visible. Here $z = 0.5$, $\phi = 0.15$, $\delta = 0.412$ and other parameter values are as in (23).

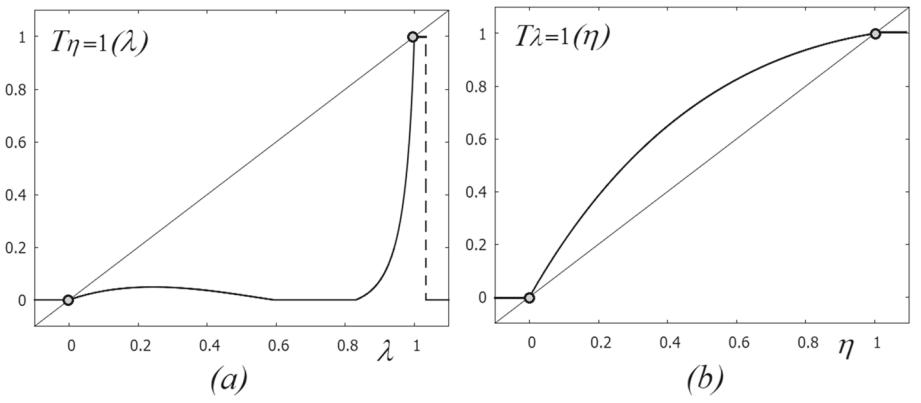

Fig. 8 1D maps $T_{\eta=1}(\lambda)$ in (**a**) and $T_{\lambda=1}(\eta)$ in (**b**) at $z = 0.5$, $\phi = 0.15$, $\delta = 0.412$. Other parameter values are as in (23)

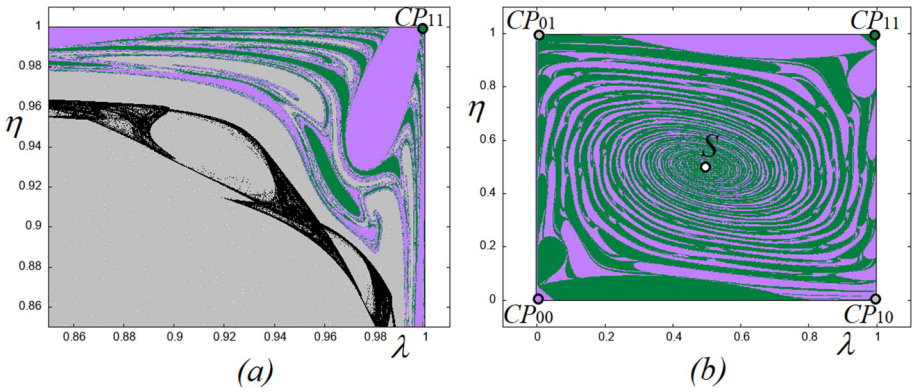

Fig. 9 **(a)** A part of the phase plane of map T where basins of attracting (in Milnor sense) fixed points CP_{00} and CP_{11} are shown in violet and green, respectively, and basin of the chaotic attractor is shown in gray; **(b)** basins of attracting fixed points CP_{00} and CP_{11}. Here $z = 0.5$, $\phi = 0.15$, and $\delta = 0.417$ in (**a**), $\delta = 0.45$ in (**b**). The other parameter values are fixed as in (23)

fact, initial points belonging to the violet and green basins are eventually attracted to CP_{00} and CP_{11}, respectively, due to the flat branches of map T, that makes these fixed points attracting in Milnor sense. It is worth to emphasize that in any neighborhood of CP_{00} and CP_{11} there are points attracted by other attractors. For other analyses of similar attractors in NEG models we refer to Commendatore et al. (2015a, b, 2021).

A closed invariant curve (with periodic or quasiperiodic dynamics) born due to a Neimark-Sacker bifurcation of S can be destroyed leading to chaos. Several mechanisms of such a destruction are described, e.g. in Aronson et al. (1982). An example of a chaotic attractor coexisting with attracting (in Milnor sense) fixed points CP_{00} and CP_{11} is presented in Fig. 9a. In this figure, a part of the phase plane is shown where it can be seen that this chaotic attractor is near to a contact with its basin boundary. In fact, for further increasing δ such a contact occurs, after which the chaotic attractor disappears (it is transformed into a chaotic repellor) leaving two attractors, CP_{00} and CP_{11}, whose basins are very intermingled. An example is shown in Fig. 9b. However, in this figure the fixed points CP_{00} and CP_{11} are already attracting in topological sense (i.e., each of these fixed points has an attracting neighborhood) since the related parameter point is above the curve C. As illustrated in Fig. 10a, the parameter point $(\phi, \delta) = (0.15, 0.417)$ (as in Fig. 9a) is below the curve C, so that the vertical asymptote $\lambda = \lambda_a$ of function f given in (31) is still outside the unit interval (see Fig. 10a), and the fixed point $\lambda = 1$ of map $T_{\eta=1}(\lambda)$ is left-side repelling. In contrast, parameter point $(\phi, \delta) = (0.15, 0.45)$ (as in Fig. 9b) is above the curve C, and the asymptote $\lambda = \lambda_a$ of f is already inside the unit interval (see Fig. 10b). As a result, the fixed point $\lambda = 1$ of map $T_{\eta=1}(\lambda)$ is both-side superstable. However, this map is no longer continuous on the unit interval as it is in the former case.

To end our discussion of the dynamics of map T at $z = 0.5$, we show in Fig. 11 a time path for different attractors: an invariant curve in (**a**), a cycle in (**b**) and a chaotic attractor in (**c**). We found, in simulations not presented here, similar time paths for other values of the parameter z (in particular, for $z = 1$ and $z = 2$).

The basic bifurcation scenario for $z = 2$ observed after a Neimark-Sacker bifurcation is qualitatively similar to the one described above for $z = 0.5$. After a Neimark-Sacker bifurcation of the fixed point S an attracting closed invariant curve is born and then it is destroyed that leads to chaos, moreover, attractors associated with this scenario may coexist

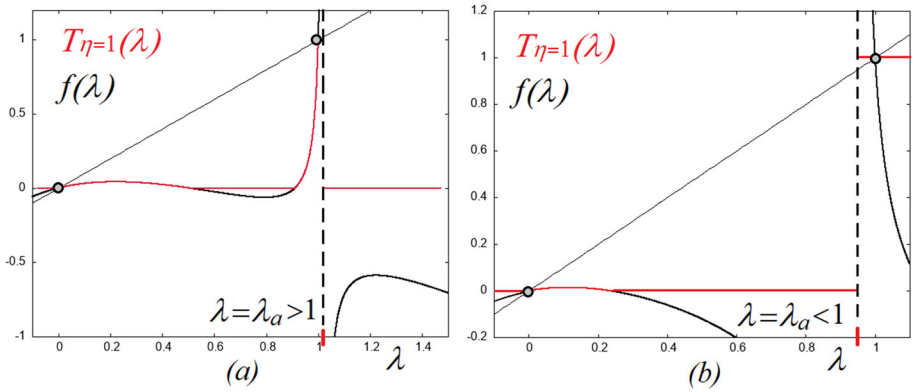

Fig. 10 Functions $f(\lambda)$ (in black) and $T_{\eta=1}(\lambda)$ (in red) and their vertical asymptote. Here $z = 0.5$, $\phi = 0.15$, and $\delta = 0.417$ in (**a**), $\delta = 0.45$ in (**b**). The other parameter values are fixed as in (23)

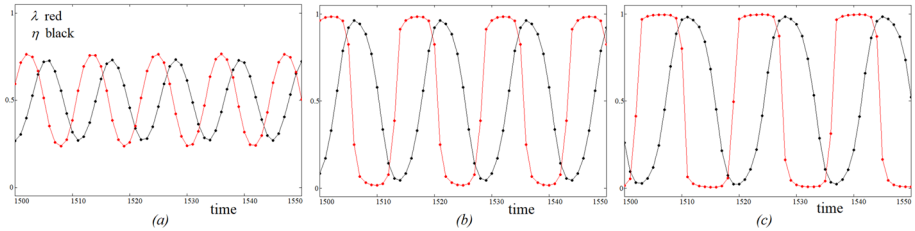

Fig. 11 Time paths followed by the share of mobile households (entrepreneurs), λ, in red and the share of firms, η, in black; for $z = 0.5$, $\phi = 0.15$ and (**a**) $\delta = 0.38$, (**b**) $\delta = 0.412$, (**c**) $\delta = 0.417$. The other parameter values are as in (23)

with attracting fixed points CP_{00} and CP_{11}. Figure 12a shows the bifurcation structure in the (ϕ, δ)-parameter plane, and in Fig. 12b a 1D bifurcation diagram is presented illustrating the dynamics of map T after the Neimark-Sacker bifurcation of the fixed point S. Note that the related parameter path (marked in Fig. 12a by a red arrow) is above the curve C, that is, interior attractors of T coexist with attracting fixed points CP_{00} and CP_{11}. Two examples are shown in Fig. 13: in (a) basins of coexisting attracting closed invariant curve and fixed points CP_{00} and CP_{11}, and in (b) basins of CP_{00} and CP_{11}.

4.5 Economic interpretation

In NEG models two types of countervaling dynamic forces are at work: spatial agglomeration and dispersion forces. Typically, in NEG models, which are mostly one-dimensional and set in continuous time, these forces are mainly considered when operating at the symmetric equilibrium. A crucial difference compared with the standard NEG analysis is that in the current set-up it is possible to distinguish which specific forces affect industry location and residence choices. The Jacobian (see expression (24) in the Appendix) nicely allows to disentangle the agglomeration and dispersion forces at work:

$$J = \begin{bmatrix} 1 + \gamma_\lambda \frac{\partial \Omega(\lambda,\eta)}{\partial \lambda} & \gamma_\lambda \lambda \frac{\partial \Omega(\lambda,\eta)}{\partial \eta} \\ \gamma_\eta \eta \frac{\partial \Psi(\lambda,\eta)}{\partial \lambda} & 1 + \gamma_\eta \frac{\partial \Psi(\lambda,\eta)}{\partial \eta} \end{bmatrix}$$

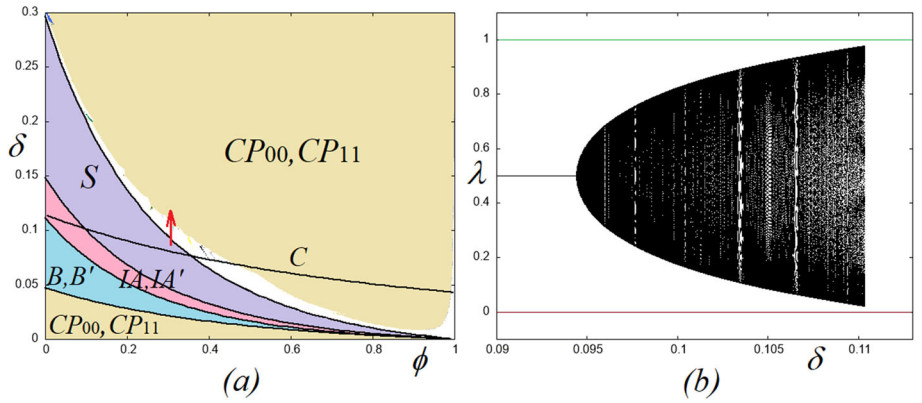

Fig. 12 (**a**) Bifurcation structure in the (ϕ, δ)-parameter plane of map T for $z = 2$. (**b**) 1D bifurcation diagram δ versus λ for $\phi = 0.3$ and $0.09 < \delta < 0.113$ (the related parameter path is marked by red arrow in (**a**)). The other parameter values are fixed as in (23)

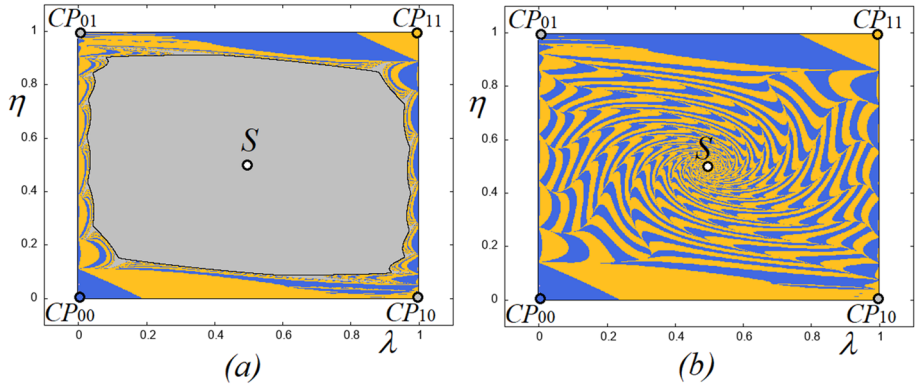

Fig. 13 (**a**) Basins of coexisting attracting closed invariant curve and fixed points CP_{00}, CP_{11} are shown in gray, yellow and blue, respectively. (**b**) After a contact with its basin boundary the interior attractor disappears, leaving only attracting fixed points CP_{00}, CP_{11}. Here $z = 2$, $\phi = 0.3$, $\delta = 0.11$ in (**a**) and $\delta = 0.12$ in (**b**). The other parameter values are fixed as in (23)

For the symmetric equilibrium S of the current model we have:

$$\left.\frac{\partial \Omega(\lambda,\eta)}{\partial \lambda}\right|_{\lambda=0.5,\ \eta=0.5} = \underbrace{\frac{-\delta \dfrac{\frac{(0.5\kappa_2)^{1+z}}{\kappa_3}}{\kappa_4 - \delta \frac{(0.5\kappa_2)^{1+z}}{1+z}}}_{indirect\ pollution\ effect\ (-)}$$

$$\left.\frac{\partial \Omega(\lambda,\eta)}{\partial \eta}\right|_{\lambda=0.5,\ \eta=0.5} = \underbrace{\frac{\kappa_1}{\kappa_4 - \delta \frac{(0.5\kappa_2)^{1+z}}{1+z}}}_{cost\ of\ living\ effect\ (+)} \underbrace{\frac{-2\delta \dfrac{(0.5\kappa_2)^{1+z}}{\kappa_4 - \delta \frac{(0.5\kappa_2)^{1+z}}{1+z}}}_{direct\ pollution\ effect\ (-)}$$

$$\left.\frac{\partial \Psi(\lambda,\eta)}{\partial \lambda}\right|_{\lambda=0.5,\ \eta=0.5} = \underbrace{\frac{1}{\kappa_3}}_{market\ size\ effect\ (+)}$$

$$\left.\frac{\partial \Psi(\lambda,\eta)}{\partial \eta}\right|_{\lambda=0.5,\ \eta=0.5} = \underbrace{0}_{market\ competition\ effect\ (0)}$$

According to these expressions at the symmetric equilibrium, the agglomeration forces are spurred by the market size effect, according to which firms are attracted by larger markets and by the cost of living effect, according to which households prefer to live where the availability of the good varieties is larger. Concerning the dispersion forces, the competition effect, according to which firms prefer to locate where the competition is less fierce, is not operative, since demand cross elasticities are nil. In passing, we notice that in Rauscher (2009) there is a further dispersion force operating at the symmetric equilibrium, involving households, according to which a higher share of households λ determines higher local prices by increasing demand. When $\delta > 0$, pollution introduces additional dispersion forces, since households prefer a less polluted environment. In the current set-up two pollution effects are present: 1) a direct pollution effect, which operates via η: when the number of firms increases the amount of local pollution increases as well; 2) an indirect pollution effect, which operates via λ: when the number of households increases, the market size increases, production increases and pollution increases (this indirect effect of pollution is missing in Rauscher 2009).

These forces also allow an economic interpretation of a "chase-and-flee" dynamics that may involve firms and households: If the symmetric equilibrium is shocked by an exogenous relocation of households towards region 1 (λ increases), firms will follow (market size effect), but some of the households will flee (because of the indirect pollution effect). With a higher number of firms in region 1, households experience a cost of living effect (attracting households to region 1) and a direct pollution effect (driving households away from region 1). Depending upon parameters (see below), the net effect may be negative, the market size in region 1 shrinks and firms follow households towards region 2. With a sufficiently strong shock, the dynamics may leave the basin of attraction of the symmetric equilibrium and a new long-run pattern is established.[7] It is interesting to compare the forces operating at the symmetric equilibrium with those working at a border equilibrium, in wich all firms are agglomerated in one region (in the following we assume this to be region 1), but households are regionally dispersed. The dynamics of the households (captured in the first line of the Jacobian J) is still governed by an indirect pollution effect, by the cost of living effect and by the direct pollution effect. However, the forces impacting upon firm location (captured in the second line of the Jacobian J) do change. Firms are agglomerated in the region in which the remuneration of human capital is higher; there is no factor price equalisation at border equilibria and firms' decisions are not "at the margin". In this situation, a marginal relocation of households (change in λ) is too small to trigger a relocation of firms – thus, we do not observe a market size effect, $\left.\frac{\partial \Psi(\lambda,\eta)}{\partial \lambda}\right|_{\lambda=\lambda^{**},\ \eta=1} = 0$. Only a bigger shock in λ may trigger a movement. Consider now a shock in η that induces some firms to move to the other region with the lower remuneration rate. While this does not change the remuneration rates

[7] Considering for example the case of Fig. 2b, a sufficiently large shock could shift the dynamics from the basin of attraction of the symmetric equilibrium S to the basin of attraction of the border equilibrium B. If the relocation of households in region 1 is sufficiently large, due to the market size effect, all firms will move sooner or later to region 1. Initially, as the number of firms located in region 1 increases, households move back to region 2 since the pollution effect is larger than the cost of living effect. However, when the number of firms increases sufficiently, the cost of living effect begins to overcome the pollution effect and households move to region 1. In the new equilibrium B all firms are located in region 1 and a share of households larger than a half but smaller than one lives in region 1. The utility level of households is the same in both regions with a lower cost of living compensating for more pollution in region 1. Moreover, due to the larger market size, firms have no incentive to relocate in region 2.

themselves (there still is no competition effect), the average remuneration of human capital declines, and the region with the higher remuneration appears more attractive. In that case, $\frac{\partial \Psi(\lambda,\eta)}{\partial\ \eta}\Big|_{\lambda=\lambda^{**},\ \eta=1} = \frac{w2(\lambda)}{w1(\lambda)} - 1 < 0$, which contributes to stabilize the border equilibrium.

In the following, we discuss the transition process between stationary equilibria forced by the increase in the paremeter δ (representing the impact of pollution on utility). For an economic interpretation of the local bifucation analysis, explaining the effect of pollution on the transition between stationary equilibria, we start from CP_{11} and see what happens by increasing δ. The same conclusions apply by symmetry, if we start from CP_{00}. When $\delta = 0$ the agglomeration forces prevail over the dispersion forces and CP_{11} is attracting due to the fact that 1) the utility differential $(u_1(1,1) - u_2(1,1))$ is positive and $\frac{\partial \Omega(\lambda,\eta)}{\partial \lambda}\Big|_{\lambda=1,\ \eta=1} < 0$ and 2) the wage differential is positive $(w_1(1) - w_2(1))$ and $\frac{\partial \Psi(\lambda,\eta)}{\partial \eta}\Big|_{\lambda=1,\ \eta=1} < 0$. This implies that households are attracted where utility is higher and firms are attracted where the market size is larger. By increasing δ the pollution effect becomes active and dispersion forces increases (in particular, utility is decreasing in region 1 since all production is located in that region). As δ crosses the value $\delta = \widetilde{\delta}_3$, CP_{11} (and by symmetry CP_{00}) becomes unstable and the border equilibrium B (and by simmetry B') becomes stable. As the impact of pollution increases (both direct and indirect effect are higher), some of the households start to move from region 1 to region 2 ($\frac{d\lambda^{**}}{d\delta} < 0$) and this reduces local emissions in region 1, by reducing the size of the market in that region, balancing the higher δ. Utility in region 2 is also decreasing with λ^{**} (because the average income is decreasing in both regions), however in that region utility decreases less. Indeeed, along B (and B') the utility in the two regions converge. Concerning firms, we have still that the wage differential $(w_1(\lambda^{**}, 1) - w_2(\lambda^{**}, 1))$ is positive , since $\lambda^{**} > 0.5$, and $\frac{\partial \Psi(\lambda,\eta)}{\partial \eta}\Big|_{\lambda=\lambda^{**},\ \eta=1} < 0$. Therefore, there is not yet an incentive for firms to move to the other region. The economy starts to experience separation between the location of firms and households.

As δ is further increased, three possible results may occur depending on the value of z:

Case 1 (see also Fig. 3): $z < 1$, when δ crosses $\delta = \overline{\delta}$, the unstable interior asymmetric equilbria I (and symmetrically I') emerges. We have seen that the stable manifolds of I and I' separate the basins of attraction of B and B' from that of the interior symmetric equilibrium S. By starting from the border equilibrium B some perturbation may lead to the symmetric equilibrium S characterised by a completely different spatial industrial distribution. Since the basins of attraction of the border asymmetric equilibria shrink by increasing δ, the size of the shock needed to switch from B (or B') to S becomes smaller and smaller as the intensity of pollution increases.

These basins of attraction disappear as δ crosses $\delta = \widetilde{\delta}_2$ (at which $\lambda^{**} = 0.5$, i.e. the households are equally split between the regions) after which S is the only stable equilibrium. At the symmetric interior equilibrium, firms and households are equally split between region 1 and region 2. Firms and households are again concentrated in the same place. At the symmetric equilibrium, the forces governing the dynamics are those specified above.

Concerning global dynamics, looking at the range of values of δ above $\delta = \delta_{NS}$ two features are worth mentioning from an economic point of view:

A) Persistent "chase -and-flee" dynamics. As explained above, this is followed by firms and households, and by the shares λ and η, with firms, attracted by the size of the market, moving to the region where the number of households is higher and households, attracted by the less polluted environment (net of the less favourable cost of living), migrating to the region where the number of firms is smaller. Fig. 11 shows three possible time paths

depending on the value of δ. In Fig. 11a, δ is slightly above δ_{NS} and the shares λ and η fluctuate regularly along an invariant closed curve with η following with some lags λ; In Fig. 11b, the value of δ is such that the shares move along one of the two coexisiting 15-period cycles. What can be noticed in this case is that many households remain in the same region for some periods before moving abruptly to the other region, while firms relocation process is smoother; finally, in Fig. 11c, δ is such that λ and η move along a chaotic attractor, here the number of periods in which almost all households live in the region with less pollution extends and the switch to the region with less firms concentration is more abrupt.

B) The existence of coexisting attractors and that of complex basins bounduaries. Figure 9 illustrates very clearly the relevance of this aspect that the dynamic process can take. Due to the existence of very intermingled basins of attraction, very small differences in λ and / or η may lead to different long-run attractors, involving alternative cyclical time paths for firms and households (even though qualitatively similar) or complete concentration and agglomeration in one of the two regions.

5 Conclusions

We presented a NEG model, in which manufacturing uses entrepreneurs / skilled workers (owning human capital) and unskilled workers and generates local pollution (that does not accumulate), households enjoy utility from consuming all commodities (locally and imported variants) and suffer from local pollution, and households are split into two groups: unskilled workers that cannot migrate and work where they live; and skilled workers that can live and work in different locations (allowing for costless commuting or, in alternative, distance working) and choose also where to live.

The model is of the footloose entrepreneur variant, but involves two dynamic equations: the standard one governing the residence choice of skilled households, and another one governing where human capital is used in production. The current paper focussed on analytic results. However, many of the results are interesting from an economic perspective and lead into several policy issues:

We found a very wide range different fixed point constellations, involving also asymmetric interior fixed points. From an economic perspective, these are much more plausible than fixed points involving symmetric location or full agglomeration, as is typically found in NEG models.

We also found multiple, coexisting attractors. Though typical for NEG models, the pervasiveness of this phenomenon in our model is surprising. From an economic perspective, it underlines the fragility of spatial patterns of production, pollution and residence choice; small shocks can profoundly alter the long-run spatial patterns, that are not easily reversible. 'Lock-in' and path dependence are phenomena important not only in NEG, but in particular also in connection with environmental issues. First numerical explorations indicate that the utility levels are different in the different types of coexisting equilibria. This opens up room for policy interventions. However, a systematic policy analysis goes well beyond the scope of this paper.

We were also able to analytically describe many cyclical solutions giving rise to a 'flee-and-chase' pattern. Interestingly enough, we not only found strict periodic cyclical solutions which are always a bit implausible (given the irregularly fluctuating pattern of economic time series), but also cycles, which show the much more plausible pattern of irregular cyclicity, such as cycles generated by a Neimark-Sacker bifurcation and also chaotic attractors.

The analysis is suggestive for many interesting policy extensions. First, note that the different equilibria involve different utility levels for different groups. Utility for high-qualified workers will be equalized between the two regions via the migration process. Low qualified workers cannot move away from polluting manufacturing; their utility is not equalized between regions (and will also differ from the utility of high-qualified workers). Therefore, a first policy question concern the comparison of these equilibria. In addition, the different equilibria involve different regional distributions of production and consumption and thus different trade volumes. One might also be interested in how much pollution is actually incorporated in trade (if the location of residence and production differ) and one might like to extend the model to account for pollution generated by these trade flows. What are the policy options that could be taken on board in a model extension? Direct taxation of pollution, public spending for abatement and protection as well as tariffs accounting for pollution contained in trade flows. From the economic policy point of view, there are plenty of interesting questions, which we leave for future research.

Concerning the point of view of dynamical systems theory, we left for future work a more detailed investigation of the global dynamics depending on other parameters as well as basin structure of coexisting attractors, especially those which are attracting in Milnor sense.

Acknowledgements The authors would like to thank two anonymous referee for their valuable comments that helped to improve a previous version of this paper. The authors would like also to thank the participants to 11th Workshop Modelli Dinamici in Economia e Finanza - Dynamic Models in Economics and Finance (MDEF 2022), Urbino, Italy. Pasquale Commendatore acknowledges support within the project "The Impact of Crises on Complex Spatial Economic Systems (ICCSES)", Programma FRA 2022 - Università di Napoli 'Federico II' (DR/2022/2055 del 17/05/2022). Mauro Sodini acknowledges financial support from the Czech Science Foundation (GACR) under project 23-06282S, and an SGS research project of VŠBTUO (SP2023/19). Iryna Sushko is grateful to the University of Urbino (Italy) for the position of Visiting professor, and to colleagues and friends for their support during the Russian invasion of Ukraine; Iryna Sushko also acknowledges partial financial support within the project "Mathematical modelling of complex dynamical systems and processes caused by the state security" (Reg. No. 0123U100853).

Funding Open access funding provided by Università degli Studi di Napoli Federico II within the CRUI-CARE Agreement.

Declarations

Conflict of interest All authors declare that they have no conflicts of interest.

Appendix

In this Appendix we present the local stability analysis of the fixed points of map T.

The Jacobian of the map T given in (16) is:

$$J = \begin{bmatrix} 1+\gamma_\lambda \frac{\partial \Omega(\lambda,\eta)}{\partial \lambda} & \gamma_\lambda \lambda \frac{\partial \Omega(\lambda,\eta)}{\partial \eta} \\ \gamma_\eta \eta \frac{\partial \Psi(\lambda,\eta)}{\partial \lambda} & 1+\gamma_\eta \frac{\partial \Psi(\lambda,\eta)}{\partial \eta} \end{bmatrix} \tag{24}$$

Symmetric fixed point

The Jacobian (24) evaluated at the fixed point $S = (0.5, 0.5)$ is

$$J(S) = \begin{bmatrix} 1-\gamma_\lambda \frac{\delta \frac{1}{2\kappa_3}(0.5\kappa_2)^{1+z}}{\kappa_4 - \frac{\delta}{1+z}(0.5\kappa_2)^{1+z}} & \gamma_\lambda \frac{0.5\kappa_1 - \delta(0.5\kappa_2)^{1+z}}{\kappa_4 - \frac{\delta}{1+z}(0.5\kappa_2)^{1+z}} \\ \gamma_\eta \frac{1}{2\kappa_3} & 1 \end{bmatrix} \tag{25}$$

where $\kappa_4 = \overline{c_A} + \frac{H\alpha(1+\phi)[(\sigma-1)(E+L)+\sigma E]}{2EF\sigma(\sigma-1)} > 0$. Trace and determinant are equal to

$$\det J(S) = 1 - \gamma_\lambda \frac{1}{2\kappa_3}\left[\frac{\delta(1-\gamma_\eta)(0.5\kappa_2)^{1+z} + 0.5\gamma_\eta\kappa_1}{\kappa_4 - \frac{\delta}{1+z}(0.5\kappa_2)^{1+z}}\right]$$

$$trJ(S) = 2 - \gamma_\lambda \frac{1}{2\kappa_3}\frac{\delta(0.5\kappa_2)^{1+z}}{\kappa_4 - \frac{\delta}{1+z}(0.5\kappa_2)^{1+z}}$$

The local stability conditions are

$$1 - \det J(S) > 0 \tag{26}$$

$$1 + trJ(S) + \det J(S) > 0 \tag{27}$$

$$1 - trJ(S) + \det J(S) > 0. \tag{28}$$

When $\delta = 0$ it holds

$$\det J(S) = 1 - \gamma_\lambda \gamma_\eta \frac{\kappa_1}{4\kappa_3\kappa_4} < 1$$

$$tr(S) = 2.$$

This implies that condition (26) is always satisfied, while condition (28) is never satisfied. That is, as in Rauscher (2009), when there is no pollution (or it has no impact on utility), the interior symmetric fixed point is never stable.

Let $\delta > 0$. If $\delta < \delta_d$ and $\gamma_\eta \leq 1$, where $\delta_d = \frac{\kappa_4(1+z)}{(0.5\kappa_2)^{1+z}}$, condition (26) is always satisfied. Instead if $\delta < \delta_d$ and $\gamma_\eta > 1$, condition (26) can be written as:

$$\delta < \delta_{NS} = \frac{\gamma_\eta}{2(\gamma_\eta - 1)}\frac{\kappa_1}{(0.5\kappa_2)^{1+z}} \tag{29}$$

If $\delta > \delta_d$ and $\gamma_\eta \leq 1$, condition (26) is never satisfied. Instead if $\delta > \delta_d$ and $\gamma_\eta > 1$, condition (26) can be written as:

$$\delta > \delta_{NS}$$

When condition (26) is violated, a Neimark-Sacker bifurcation of S occurs.

If $(\delta - \delta_d)(8\kappa_3 - (z+1)(\gamma_\eta - 2)\gamma_\lambda) < 0$, condition (27) can be written as:

$$\delta < \delta_F = (1+z)\frac{0.5\gamma_\lambda\gamma_\eta\kappa_1 - 8\kappa_3\kappa_4}{(0.5\kappa_2)^{1+z}[\gamma_\lambda(\gamma_\eta - 2)(1+z) - 2\kappa_3]}$$

If $(\delta - \delta_d)(8\kappa_3 - (z+1)(\gamma_\eta - 2)\gamma_\lambda) > 0$, condition (27) can be written as:

$$\delta > \delta_F$$

When this condition is violated a flip bifurcation of S occurs.

If $\delta < \delta_d$, condition (28) can be written as

$$\delta > \frac{2^z \kappa_1}{\kappa_2^{1+z}} = \overline{\delta} \tag{30}$$

Instead, if $\delta > \delta_d$, condition (28) corresponds to

$$\delta < \overline{\delta}$$

When condition (28) is violated a pitchfork bifurcation of S occurs.

Comparing (26) and (28) when $\gamma_\eta > 1$, we have that if $\delta < \delta_d$, these conditions are simultaneously satisfied for $\overline{\delta} < \delta < \delta_{NS}$. Instead, if $\delta > \delta_d$, these conditions cannot hold simultaneously, since $\delta_{NS} > \overline{\delta}$.

Interior Asymmetric fixed points

For $\delta = \overline{\delta}$ and $z > 1 (< 1)$ a supercritical (subcritical) pitchfork bifurcation of the symmetric fixed point S takes place leading for decreasing δ (for increasing δ) to two asymmetric stable (unstable) fixed points I and I'. If $z = 1$ the pitchfork bifurcation is degenerate. Local stability properties of the fixed points I and I' for the case $z = 2$ are analyzed below in this Appendix.

Border and core-periphery fixed points

Let map T reduced to the invariant border $\{(\lambda, \eta) : 0 \leq \lambda \leq 1, \ \eta = 1\}$ be denoted by $T_{\eta=1}(\lambda)$. Its dynamics at this border is determined by the equation

$$f(\lambda, 1) = f(\lambda) = \lambda \left(1 + \gamma_\lambda (1-\lambda) \frac{u_1(\lambda) - u_2(\lambda)}{\lambda u_1(\lambda) + (1-\lambda) u_2(\lambda)}\right) \tag{31}$$

where

$u_1(\lambda) = w_1(\lambda)\frac{H}{E} + \overline{c_A} + \frac{\alpha}{\sigma - 1}\frac{H}{F} - \frac{\delta}{1+z}(H\sigma w_1(\lambda))^{1+z}$,

$u_2(\lambda) = w_1(\lambda)\frac{H}{E} + \overline{c_A} + \frac{\alpha}{\sigma - 1}\frac{H}{F}\phi$.

If $|f'(\lambda^{**})| < 1$, where $f'(\lambda^{**}) = 1 - \gamma_\lambda \lambda^{**}(1-\lambda^{**})\left(\frac{\delta\sigma E(\sigma H w_1(\lambda^{**}))^z}{u_1(\lambda^{**})}\right)$, the fixed point λ^{**} of f is stable. We have that border fixed point $B = (\lambda^{**}, 1)$ can lose stability (in the horizontal direction) via a border transcritical bifurcation at $\delta = \widetilde{\delta}_3$ exchanging stability with CP_{11} and at $\delta = \widetilde{\delta}_1$ exchanging stability with CP_{01}. By symmetry, B' is stable within the interval $\widetilde{\delta}_3 < \delta < \widetilde{\delta}_1$ exchanging stability with CP_{00} at $\delta = \widetilde{\delta}_3$ and with CP_{10} at $\delta = \widetilde{\delta}_1$.

Indeed, moving on to the entire domain of the map T, the Jacobian (24) evaluated at the border fixed point B is a diagonal matrix with the two eigenvalues lying along the main diagonal. These are

$$1 - \gamma_\lambda \lambda^{**}(1-\lambda^{**})\delta^{\frac{1}{1+z}} \frac{\kappa_2}{\kappa_3} \frac{[\kappa_1(1+z)]^{\frac{z}{1+z}}}{u_1(\lambda^{**}, 1)} < 1 \text{ for } 0 < \lambda^{**} < 1$$

that is for $\widetilde{\delta}_3 < \delta < \widetilde{\delta}_1$, and

$$1 - \gamma_\eta \frac{\kappa_0(2\lambda^{**} - 1)}{u_1(\lambda^{**}, 1)} < 1 \text{ for } \lambda^{**} > 0.5$$

that is for $\delta < \widetilde{\delta}_2$. By symmetry, the same applies to B'. Notice also that when $\delta = 0$, it holds that $f(\lambda)$ has no interior fixed point. Therefore, B and B' do not exist when $\delta = 0$.

The border fixed points B and B' can also lose stability via a flip bifurcation. It occurs when

$$\gamma_\lambda = \widetilde{\gamma}_\lambda = 2\left(\frac{u_1(\lambda^{**})}{\delta\sigma E(\sigma H w_1(\lambda^{**}))^z}\right)$$

For what is concerning the core-periphery fixed points, the Jacobian (24) evaluated at the core-periphery fixed point CP_{11} is an upper triangular matrix with the two eigenvalues lying along the main diagonal. These are:

$$1-\gamma_\lambda\frac{\widetilde{\delta}_3-\delta}{\widetilde{\delta}_3}\frac{\kappa_1}{u_1(1,1)}<1 \text{ for } \delta<\widetilde{\delta}_3$$
$$1-\gamma_\eta\frac{1}{\kappa_3+0.5}<1 \text{ always}$$

Therefore, CP_{11} (and by symmetry CP_{00}) can lose stability only along the horizontal direction when $\delta>\widetilde{\delta}_3$. Regarding the core-periphery fixed points with separation, the Jacobian evaluated at CP_{01} is also an upper triangular matrix with the two eigenvalues lying on the main diagonal. These are

$$1-\gamma_\lambda\frac{\delta-\widetilde{\delta}_1}{\widetilde{\delta}_1}\frac{\kappa_1}{u_2(0,1)}<1 \text{ for } \delta>\widetilde{\delta}_1$$
$$1+\gamma_\eta\frac{1}{\kappa_3-0.5}>1 \text{ always}$$

Therefore, CP_{01} (and by symmetry CP_{10}) loses stability along the horizontal direction when $\delta<\widetilde{\delta}_1$ and it is always unstable along the vertical direction.

Asymmetric interior fixed points for $z=2$

We consider the fixed point I, then by symmetry the same results apply to I'.

The Jacobian (24) evaluated at the asymmetric interior fixed point $I=(0.5,\eta^*)$ is

$$J(I)=\begin{bmatrix}1-\frac{\gamma_\lambda}{4u^*}\delta\frac{\kappa_2^{1+z}}{\kappa_3}\left[(\eta^*)^{1+z}+(1-\eta^*)^{1+z}\right] & -\frac{\gamma_\lambda}{4u^*}\left[\delta\left(\kappa_2^{1+z}\left[(\eta^*)^z+(1-\eta^*)^z\right]\right)-2\kappa_1\right]\\ \frac{2\gamma_\eta\eta^*(1-\eta^*)}{\kappa_3} & 1\end{bmatrix}$$

where $u^*=\kappa_4-\frac{\kappa_1}{2}\frac{1+\phi}{1-\phi}+\alpha\frac{1}{\sigma-1}\frac{H}{F}\left(\eta^*+\phi(1-\eta^*)\right)-\frac{\delta}{1+z}\left(\eta^*\kappa_2\right)^{1+z}$.

Let $z=2$. The above Jacobian becomes

$$J(I)=\begin{bmatrix}1-\frac{\gamma_\lambda}{4u^*}\frac{9\kappa_1-2\delta\kappa_2^3}{\kappa_3} & \frac{\gamma_\lambda}{4u^*}\left(\delta\kappa_2^3-4\kappa_1\right)\\ \frac{2\gamma_\eta\eta^*(1-\eta^*)}{\kappa_3} & 1\end{bmatrix}$$

where $u^*=\kappa_4-\frac{\kappa_1}{2}\frac{1+\phi}{1-\phi}+\alpha\frac{1}{\sigma-1}\frac{H}{F}\left(\eta^*+\phi(1-\eta^*)\right)-\frac{\delta}{3}\left(\eta^*\kappa_2\right)^3$ and

$$\eta^*=\frac{1}{2}+\frac{\sqrt{3\delta\kappa_2^3(4\kappa_1-\delta\kappa_2^3)}}{2\delta\kappa_2^3}$$
$$1-\eta^*=\frac{1}{2}-\frac{\sqrt{3\delta\kappa_2^3(4\kappa_1-\delta\kappa_2^3)}}{2\delta\kappa_2^3}$$

Notice that the asymmetric solutions are real and distinct and $\frac{1}{2}<\eta^*<1$ for $\frac{3\kappa_1}{\kappa_2^3}=\widetilde{\delta}_2<\delta<\frac{4\kappa_1}{\kappa_2^3}=\overline{\delta}$.

The stability conditions are:

$$1 - \det J\,(I) > 0 \tag{32}$$

$$1 + trJ\,(I) + \det J\,(I) > 0 \tag{33}$$

$$1 - trJ\,(I) + \det J\,(I) > 0 \tag{34}$$

To verify when these conditions hold we proceed as follows. Condition (32) corresponds to:

$$\frac{2\kappa_2^6(\gamma_\eta - 1)\delta^2 - \kappa_1\kappa_2^3(14\gamma_\eta - 9)\delta + 24\kappa_1^2\gamma_\eta}{4\delta\kappa_2^3\kappa_3 u^*} > 0$$

The sign of this expression depends on that of the numerator. For $\gamma_\eta > 1 (< 1)$ the numerator in this expression corresponds to a parabola with a minimum (maximum). The intersection points of this parabola with the horizontal axis are $\delta_a = \frac{\kappa_1}{\kappa_2^3}\frac{14\gamma_\eta - 9 - \sqrt{\left(\gamma_\eta - \frac{3}{2}\right)\left(\gamma_\eta - \frac{27}{2}\right)}}{\gamma_\eta - 1}$ and $\delta_b = \frac{\kappa_1}{\kappa_2^3}\frac{14\gamma_\eta - 9 + \sqrt{\left(\gamma_\eta - \frac{3}{2}\right)\left(\gamma_\eta - \frac{27}{2}\right)}}{\gamma_\eta - 1}$. Looking at the numerator, we can say that:

1. When $\gamma_\eta > \frac{27}{2}$ it is positive for $\delta < \delta_a$ and for $\delta > \delta_b$, with $\delta_a < \delta_b < \overline{\delta}$.
2. When $\gamma_\eta = \frac{27}{2}$ it is positive for $\delta \neq \delta_a = \delta_b = \frac{18\kappa_1}{5\kappa_2^3} < \overline{\delta}$.
3. When $\frac{3}{2} < \gamma_\eta < \frac{27}{2}$ it is positive for any δ.
4. When $\gamma_\eta = \frac{3}{2}$ it is positive for $\delta \neq \delta_a = \delta_b = \frac{6\kappa_1}{\kappa_2^3} > \overline{\delta}$.
5. When $1 < \gamma_\eta < \frac{3}{2}$ it is positive for $\delta < \delta_a$ and for $\delta > \delta_b$, with $\overline{\delta} < \delta_a < \delta_b$.
6. When $\gamma_\eta = 1$ it is positive for $\delta > \frac{24\kappa_1}{5\kappa_2^3} > \overline{\delta}$.
7. When $0 < \gamma_\eta < 1$ it is positive for $\delta_b < 0 < \delta < \overline{\delta} < \delta_a$.

From points 1-7 we conclude that, when $\gamma_\eta < \frac{27}{2}$ condition (32) is satisfied as long as $\delta < \overline{\delta}$ and when $\gamma_\eta \geq \frac{27}{2}$ it is satisfied for $\delta_b < \delta < \overline{\delta}$.

Condition (33) corresponds to:

$$4 - \gamma_\lambda\frac{9\kappa_1 - 2\delta\kappa_2^3}{2\kappa_3 u^*} - \gamma_\lambda\gamma_\eta\frac{(4\kappa_1 - \delta\kappa_2^3)(3\kappa_1 - \delta\kappa_2^3)}{2\delta\kappa_2^3\kappa_3 u^*} > 0$$

Noticing that from the inequalities $\widetilde{\delta}_2 < \delta < \overline{\delta}$ it follows $(4\kappa_1 - \delta\kappa_2^3)(3\kappa_1 - \delta\kappa_2^3) < 0$, condition (33) holds when

$$\gamma_\eta > \gamma_{\eta Fl}^A = \frac{\delta\kappa_2^3\left[8\kappa_3 u^* - \gamma_\lambda(9\kappa_1 - 2\delta\kappa_2^3)\right]}{\gamma_\lambda(4\kappa_1 - \delta\kappa_2^3)(3\kappa_1 - \delta\kappa_2^3)}$$

Finally, condition (34) corresponds to:

$$\frac{\gamma_\lambda\gamma_\eta(4\kappa_1 - \delta\kappa_2^3)(3\kappa_1 - \delta\kappa_2^3)}{2\delta\kappa_2^3\kappa_3 u^*} < 0$$

This condition holds when $\widetilde{\delta}_2 < \delta < \overline{\delta}$. At $\delta = \widetilde{\delta}_2$ the fixed points I and I' lose stability and disappear via a border transcritical bifurcation, while at $\delta = \overline{\delta}$ they disappear via a reverse pitchfork bifurcation.

References

Aronson, D. G., Chory, M. A., Hall, G. R., & McGehee, R. P. (1982). Bifurcations from an invariant circle for two-parameter families of maps of the plane: A computer-assisted study. *Communications in Mathematical Physics, 83*, 303–354.

Borck, R., & Pflüger, M. (2019). Green cities? Urbanization, trade, and the environment. *Journal of Regional Science, 59*(4), 743–766.

Borck, R., Pflüger, M., & Wrede, M. (2010). A simple theory of industry location and residence choice. *Journal of economic geography, 10*(6), 913–940.

Chen, S., Oliva, P., & Zhang, P. (2022). The effect of air pollution on migration: Evidence from China. *Journal of Development Economics, 156*, 102833.

Ciucci, J., Prunetti, D., & Maupertuis, M. A. (2015). Spatial distribution of economic activities and transboundary pollutions. *International Journal of Sustainable Development, 18*(1–2), 77–93.

Commendatore, P., Kubin, I., & Sushko, I. (2015b). Typical bifurcation scenario in a three region identical new economic geography model. *Mathematics and Computers in Simulation, 108*, 63–80.

Commendatore, P., Kubin, I., & Sushko, I. (2021). A propos Brexit: On the breaking up of integration areas – an NEG analysis. *Spatial Economic Analysis, 16*(1), 97–120.

Commendatore, P., Kubin, I., Mossay, P., & Sushko, I. (2015a). Dynamic agglomeration patterns in a two-country new economic geography model with four regions. *Chaos, Solitons & Fractals, 79*, 2–17.

Forslid, R., & Ottaviano, G. I. (2003). An analytically solvable core-periphery model. *Journal of Economic Geography, 3*(3), 229–240.

Fujita, M., Krugman, P. R., & Venables, A. (1999). The spatial economy: Cities, regions, and international trade. MIT press.

Gaspar, J. M. (2018). A prospective review on New Economic Geography. *The Annals of Regional Science, 61*(2), 237–272.

Gaigné, C., Riou, S., & Thisse, J. F. (2012). Are compact cities environmentally friendly? *Journal of Urban Economics, 72*(2–3), 123–136.

Germani, A. R., Scaramozzino, P., Castaldo, A., & Talamo, G. (2021). Does air pollution influence internal migration? An empirical investigation on Italian provinces. *Environmental Science & Policy, 120*, 11–20.

Heblich, S., Trew, A., & Zylberberg, Y. (2021). East-side story: Historical pollution and persistent neighborhood sorting. *Journal of Political Economy, 129*(5), 1508–1552.

Krugman, P. (1991). Increasing returns and economic geography. *Journal of Political Economy, 99*(3), 483–499.

Krugman, P. (1993). First nature, second nature, and metropolitan location. *Journal of Regional Science, 33*(2), 129–144.

Levine, R., Lin, C., & Wang, Z. (2018). Pollution and human capital migration: Evidence from corporate executives (No. w24389). National Bureau of Economic Research.

Li, X., Chen, H., & Li, Y. (2020). The effect of air pollution on children's migration with parents: Evidence from China. *Environmental Science and Pollution Research, 27*, 12499–12513.

Lange, A., & Quaas, M. F. (2007). Economic geography and the effect of environmental pollution on agglomeration. *The BE Journal of Economic Analysis & Policy*, *7*(1).

Martínez-García, P., Morales, J. R., & Caballero, M. V. (2022). Pollution-Induced Migration and Environmental Policy. No Half Measures. Available at SSRN: https://ssrn.com/abstract=4284479

Michel, P., & Rotillon, G. (1995). Disutility of pollution and endogenous growth. *Environmental and Resource Economics, 6*, 279–300.

Milnor, J. (1985). On the concept of attractor. *Communications in Mathematical Physics, 99*, 177–195.

OECD. (2016). The Economic Consequences of Outdoor Air Pollution. *OECD Publishing, Paris.* https://doi.org/10.1787/9789264257474-en

Ottaviano, G. I. (2001). Monopolistic competition, trade, and endogenous spatial fluctuations. *Regional Science and Urban Economics, 31*(1), 51–77.

Pflüger, M. (2021). City size, pollution and emission policies. *Journal of Urban Economics, 126*, 103391.

Rauscher, M. (2009). Concentration, separation, and dispersion: Economic geography and the environment. Thünen-series of applied economic theory, 109.

Rauscher, M., & Barbier, E. B. (2010). Biodiversity and geography. *Resource and Energy Economics, 32*(2), 241–260.

Sushko, I., & Gardini, L. (2010). Degenerate bifurcations and border collisions in piecewise smooth 1D and 2D maps. *International Journal of Bifurcation and Chaos, 20*(07), 2045–2070.

Tiebout, C. M. (1956). A pure theory of local expenditures. *Journal of political economy, 64*(5), 416–424.

van Marrewijk, C. (2005). Geographical Economics and the Role of Pollution on Location. *ICFAI Journal of Environmental Economics, 3*, 28–48.

Weibull, J. W. (1995). Evolutionary game theory. MIT press.
Xu, X., & Sylwester, K. (2016). Environmental quality and International migration. *Kyklos, 69*(1), 157–180.
Xue, S., Zhang, B., & Zhao, X. (2021). Brain drain: The impact of air pollution on firm performance. *Journal of Environmental Economics and Management, 110*, 102546.
Zeng, D. Z., & Zhao, L. (2009). Pollution havens and industrial agglomeration. *Journal of Environmental Economics and Management, 58*(2), 141–153.